Numer. Math. Theor. Meth. Appl. doi: 10.4208/nmtma.OA-2024-0086

Analysis and Efficient Implementation of Quadratic Spline Collocation ADI Methods for Variable-Order Time-Fractional Mobile-Immobile Diffusion Equations

Jun Liu¹, Hongfei Fu^{2,3,*}, Bingyin Zhang² and Jiansong Zhang¹

Received 25 July 2024; Accepted (in revised version) 3 December 2024

Abstract. In this paper, a quadratic spline collocation (QSC) method combined with L1 time discretization in the framework of alternating direction implicit (ADI) approach, namely ADI-QSC-L1 method, is developed to solve the variable-order time-fractional mobile-immobile diffusion equations in multi-dimensional spaces. Discrete L_2 norm-based stability and error estimate are carefully discussed, which show that the proposed method is unconditionally stable and convergent with first-order accuracy in time and second-order accuracy in space. Then, based on the exponential-sum-approximation technique for the fast evaluation of the variable-order Caputo fractional derivative, an efficient implementation strategy of the ADI-QSC-L1 method, named ADI-QSC-L1 is presented, which further improves the computational efficiency by reduced memory requirement and computational cost. Finally, numerical examples are provided to support both the theoretical results and efficiency of the developed method.

AMS subject classifications: 65M12, 65M15, 65M70

Key words: Time-fractional mobile-immobile diffusion equations, variable-order, QSC method, ADI, stability and convergence, fast implementation.

1. Introduction

A large number of research indicates that many natural phenomena and structures can be better described by fractional differential equations (FDEs), due to the histori-

¹ College of Science, China University of Petroleum (East China), Qingdao 266580, China

² School of Mathematical Sciences, Ocean University of China, Qingdao 266100, China

³ Laboratory of Marine Mathematics, Ocean University of China, Qingdao 266100, China

^{*}Corresponding author. *Email addresses*: liujun@upc.edu.cn (J. Liu), fhf@ouc.edu.cn (H. Fu), zhangbingyin@stu.ouc.edu.cn (B. Zhang), jszhang@upc.edu.cn (J. Zhang)

cal memory and global correlation of the fractional operators, such as fluid flow in an unsaturated media [32,36], viscoelastic anomalous diffusion in complex liquids [30], chemical reactions in underground water and so on [37]. In recent years, the time-FDEs, which are often used to describe the subdiffusive solutes transport in heterogeneous media [31,34,46] or model the memory behavior of shape-memory polymer [17], have attracted great interests of researchers. Wang and Zheng [40] developed a modified two-scale variable-order time-fractional mobile-immobile equation to model the solute transport in heterogeneous porous media, and they rigorously proved the wellposedness and regularity of the model.

It is well-known that numerical modeling is one of the main methods for solving many types of FDEs, and indeed various numerical methods have been developed, such as finite difference methods [1, 9, 14, 20, 28, 35, 38, 39, 51], finite element methods [3, 13, 15, 26, 43, 48], finite volume methods [7, 8, 49], spectral methods [2, 44]. As an efficient numerical tool, quadratic spline collocation (OSC) methods have been successfully studied for integer-order differential equations [4,5,10], and have also been applied for FDEs, for example, Luo et al. [27] proposed a space-time QSC method in all-at-once manner to solve the sub-diffusion equations. We combined the QSC method and L1 formula for solving the sub-diffusion equation with fractional boundary conditions, and rigorous numerical analysis is given in [24]. Besides, we also developed and analyzed the QSC method for space-FDEs [22, 23, 25]. Moreover, some other types of collocation methods for FDEs are also considered, see [16, 18, 42]. Recently, the authors applied the QSC method for variable-order time-fractional mobile-immobile diffusion equations with variably diffusive coefficients [21], and showed that the method is unconditionally stable and convergent with first-order in time and second-order in space with respect to some discrete and continuous L_2 norms. Then, combined with the reduced basis technique, an efficient QSC-L1-RB method was proposed to further improve the computational efficiency. This seems the first paper on analysis of QSC method for variable-order time-fractional model. However, for large-scale and long time modeling and simulations, the method is still computationally expensive. Therefore, it deserves to develop much more efficient numerical methods for the interested two-scale variable-order model.

Alternating direction implicit (ADI) method, serving an operator spitting method, is able to convert the multi-dimensional large-scale problem into a series of one-dimensional small-scale subproblems. Thus, it can reduce the computational cost greatly and solve the model problem easily in parallel. Various ADI methods have been extensively developed for time-FDEs [6,41,47]. Another efficient approach for time-FDEs is the sum-of-exponentials (SOE) technique. Jiang et al. [12] proposed a fast evaluation method for the constant-order Caputo fractional derivative by the SOE approximation. This method is able to reduce the memory requirement and the computational cost greatly. However, it can not be directly applied to the variable-order fractional derivative and related model. Recently, Zhang et al. [45] provided a variant SOE technique, named exponential-sum-approximation (ESA), to approximate the variable-order Caputo fractional derivative and variable-order time-fractional diffusion equation. In this

paper, we will put forward an efficient numerical method from both time and space approximation angles, for the variable-order time-fractional mobile-immobile diffusion equations, and our contributions are mainly threefold:

- Combining the QSC method in ADI framework and the L1 temporal discretization formula, we developed an efficient ADI-QSC-L1 method for multi-dimensional variable-order time-fractional mobile-immobile diffusion equations, where nonhomogeneous boundary equations for the homogeneous Dirichlet boundary conditions are treated technically in the ADI approach.
- ullet Discrete L_2 norm-based unconditionally stability and convergence analysis of the ADI-QSC-L1 method are rigorously discussed, and the result is proved to be firstorder accurate in time and second-order accurate in space. Furthermore, we also discuss an efficient implementation of the ADI-QSC-L1 method by the ESA technique to further reduce the computational cost.
- · Numerical experiments for two- and three-dimensional variable-order time-fractional models are presented to illustrate the convergence and efficiency of the proposed ADI methods. Moreover, an adaptive temporal stepsize strategy is considered for the ADI-QSC-L1 approximation of the variable-order time-fractional Allen-Cahn equation, and comparisons of the computational efficiency with the direct method on uniform temporal grids are tested.

The outline of the paper is organized as follows. In Section 2, we first propose the ADI-OSC-L1 method for the variable-order time-fractional mobile-immobile diffusion equation in two space dimensions, and then analyze the stability and convergence of the method in Section 3. Efficient implementation of the ADI-QSC-L1 method based on the ESA technique is briefly discussed in Section 4. Three numerical experiments are provided in Section 5 to verify the convergence and efficiency of the proposed methods. Finally, concluding remarks are given in the last section.

2. Variable-order time-FDE and the ADI-QSC-L1 approximation

In this section, we consider the following variable-order time-FDE:

this section, we consider the following variable-order time-FDE:
$$\begin{cases} \partial_t u(X,t) + \lambda_0^C \mathcal{D}_t^{1-\alpha(t)} u(X,t) = D\Delta u(X,t) + f(X,t) & \text{in } \Omega \times I, \\ u(X,t) = \varphi(X,t) & \text{on } \partial\Omega \times I, \\ u(X,0) = u^o(X) & \text{in } \Omega, \end{cases} \tag{2.1}$$

where I := (0,T], $\Omega := (x_L,x_R) \times (y_L,y_R)$ is a rectangular domain with sizes $L_1 =$ $x_R - x_L, L_2 = y_R - y_L, \partial \Omega$ denotes the boundary of $\Omega, X = (x, y)$. The diffusion coefficient matrix $D=\mathrm{diag}\{d_1,d_2\}$ with d_1 and d_2 being positive constants. Besides, λ is a positive capacity constant, f and u^o are prescribed source and initial functions. Here, we assume $\alpha \in C^1[0,T]$, and it satisfies the following conditions:

$$0 < \alpha_* := \min_{t \in [0,T]} \alpha(t) \le \max_{t \in [0,T]} \alpha(t) := \alpha^* < 1, \quad \lim_{t \to 0+} \left(\alpha(t) - \alpha(0) \right) \ln t \quad \text{exists.} \quad (2.2)$$

The variable-order Caputo fractional derivative is defined by

$${}_{a}^{C}\mathcal{D}_{t}^{1-\alpha(t)}g(t) := \left[\frac{1}{\Gamma(\alpha(t))} \int_{a}^{\xi} \partial_{s}g(s)(\xi-s)^{\alpha(t)-1}ds\right]\bigg|_{\xi=t}.$$

Eq. (2.1) can be used to model the process of solute transport in soil [31, 46], and the first-order temporal derivative term in (2.1) represents the linear drift of time for the solute particles in the mobile phase, while the fractional-order derivative term describes the solute transport in the immobile phase, which is limited by soil structure and adsorption. The structure and porosity of soil usually depend on the previous period of rainfall or irrigation, and this historical memory can be reflected by the fractional-order operators in the mathematical model. Moreover, it is well known that, the constant-order time-FDEs suffer initial singularity. However, as reported in [50] that the variable-order time-FDE (2.1) is well-posed if conditions (2.2) and suitable smoothness assumptions on the given data are satisfied, and the initial singularity can be resolved. Throughout the paper, we assume f and u^o are sufficiently smooth.

2.1. The QSC-L1 approximation

In the following, we first consider the L1 discretization in time for problem (2.1). Let N_t be a positive integer and define a uniform temporal partition $0=t_0 < t_1 < \cdots < t_{N_t} = T$ with time stepsize $\tau = T/N_t$. At each time level t_n , we denote $\alpha_n := \alpha(t_n)$, and the temporal derivatives $\partial_t u(X,t_n)$ and ${}^C_0 \mathcal{D}^{1-\alpha_n}_t u(X,t_n)$ are respectively discretized as

$$\partial_{t}u(X,t_{n}) = \frac{1}{\tau} \left(u(X,t_{n}) - u(X,t_{n-1}) \right) + \frac{1}{\tau} \int_{t_{n-1}}^{t_{n}} \partial_{tt}u(X,t)(t-t_{n-1})dt$$

$$=: \delta_{\tau}u(X,t_{n}) + r_{1,n}, \tag{2.3}$$

$${}^{C}\mathcal{D}_{t}^{1-\alpha_{n}}u(X,t_{n}) = \frac{1}{\Gamma(\alpha_{n})} \sum_{k=1}^{n} \left[\int_{t_{k-1}}^{t_{k}} \frac{\delta_{\tau}u(X,t_{k})}{(t_{n}-t)^{1-\alpha_{n}}} dt + \int_{t_{k-1}}^{t_{k}} \frac{\partial_{t}u(X,t) - \delta_{\tau}u(X,t_{k})}{(t_{n}-t)^{1-\alpha_{n}}} dt \right]$$

$$= \frac{1}{\Gamma(1+\alpha_{n})} \sum_{k=1}^{n} b_{k}^{(n)} \left(u(X,t_{k}) - u(X,t_{k-1}) \right)$$

$$+ \frac{1}{\Gamma(\alpha_{n})} \sum_{k=1}^{n} \int_{t_{k-1}}^{t_{k}} \frac{1}{\tau(t_{n}-t)^{1-\alpha_{n}}} \left[\int_{t_{k-1}}^{t_{k}} \int_{s}^{t} \partial_{tt}u(X,\theta) d\theta ds \right] dt$$

$$=: \delta_{\tau}^{1-\alpha_{n}}u(X,t_{n}) + r_{2,n}, \tag{2.4}$$

where the coefficients

$$b_k^{(n)} = \frac{1}{\tau} [(t_n - t_{k-1})^{\alpha_n} - (t_n - t_k)^{\alpha_n}], \quad 1 \le k \le n$$

and satisfy

$$\begin{cases}
\tau^{\alpha_n - 1} = b_n^{(n)} > b_{n-1}^{(n)} > \dots > b_k^{(n)} > \dots > b_1^{(n)} > 0, \\
\alpha_n (t_n - t_{k-1})^{\alpha_n - 1} \le b_k^{(n)} \le \alpha_n (t_n - t_k)^{\alpha_n - 1}.
\end{cases}$$
(2.5)

As proved in [50, Lemma 3.1], if $\alpha(0) = 1$, the following estimates hold for $r_{1,n}$ in (2.3) and $r_{2,n}$ in (2.4)

$$||r_{1,n}||_{L^{\infty}} \le QN_t^{-1} = Q\tau, \quad ||r_{2,n}||_{L^{\infty}} \le QN_t^{-1} = Q\tau, \quad 1 \le n \le N_t,$$
 (2.6)

otherwise, if $\alpha(0) < 1$, the following estimates hold

$$||r_{1,n}||_{L^{\infty}} \le Qn^{-\alpha(0)}N_t^{\alpha(0)-1}, \quad ||r_{2,n}||_{L^{\infty}} \le Qn^{-\alpha^*}N_t^{\alpha^*-1}, \quad 1 \le n \le N_t.$$
 (2.7)

Here and what follows, Q with or without subscripts is a positive constant independent of the mesh parameters, but may have different values at different circumstances.

Next, for the spatial discretization, we employ the well-known QSC approximation. Let N_x and N_y be two positive integers, and define a uniform partition $\Delta := \Delta_x \times \Delta_y$ of Ω as

$$\Delta_x := \{ x_L = x_0 < x_1 < \dots < x_{N_x} = x_R \},$$

$$\Delta_y := \{ y_L = y_0 < y_1 < \dots < y_{N_y} = y_R \}$$

with mesh sizes $\Delta x = (x_R - x_L)/N_x$ and $\Delta y = (y_R - y_L)/N_y$. Let $h := \max\{\Delta x, \Delta y\}$. Define the index sets

$$\bar{\omega} = \{(i,j) \mid 0 \le i \le N_x + 1, \ 0 \le j \le N_y + 1\},\$$

$$\omega = \{(i,j) \mid 1 \le i \le N_x, \ 1 \le j \le N_y\}$$

and $\partial \omega = \bar{\omega} \setminus \omega$. Moreover, let $\mathcal{M} := \mathcal{M}_x \otimes \mathcal{M}_y$ be the space of piecewise biquadratic polynomials with respect to Δ such that

$$\mathcal{M}_x := \left\{ v \in C^1(x_L, x_R) : v|_{[x_{j-1}, x_j]} \in \mathbb{P}^2(x), 1 \le j \le N_x \right\},$$

$$\mathcal{M}_y := \left\{ v \in C^1(y_L, y_R) : v|_{[y_{k-1}, y_k]} \in \mathbb{P}^2(y), 1 \le k \le N_y \right\},$$

where $\mathbb{P}^2(\cdot)$ represent the set of quadratic polynomials with respect to a single variable. Note that the basis functions for the space \mathcal{M}_x is defined as

$$\phi_j(x) = \phi\left(\frac{x - x_L}{\Delta x} - j + 2\right), \quad j = 0, 1, \dots, N_x + 1,$$

where

$$\phi(x) = \frac{1}{2} \begin{cases} x^2, & 0 \le x \le 1, \\ -2(x-1)^2 + 2(x-1) + 1, & 1 \le x \le 2, \\ (3-x)^2, & 2 \le x \le 3, \\ 0, & \text{elsewhere.} \end{cases}$$

Thus, the basis functions for \mathcal{M} are defined as the tensor products of the basis functions for the spaces \mathcal{M}_x and \mathcal{M}_y . Therefore, for each $n=0,1,\ldots,N_t$, the quadratic spline solution $U^n(X)\in\mathcal{M}$ can be represented as

$$U^{n}(X) = \sum_{i=0}^{N_{x}+1} \sum_{j=0}^{N_{y}+1} c_{i,j}^{n} \phi_{i}(x) \phi_{j}(y),$$
(2.8)

where $\{c_{i,j}^n\}$ are to be determined below.

At each time level t_n , we approximate (2.1) using formula (2.3)-(2.4) and (2.8), and then taking values of the resulting equations at the collocation points

$$\Delta_c := \left\{ X_{i,j} = (\xi_i^x, \xi_j^y), \ \xi_0^x = x_L, \ \xi_i^x = (x_{i-1} + x_i)/2, \ i = 1, \dots, N_x, \ \xi_{N_x+1}^x = x_R, \right.$$

$$\xi_0^y = y_L, \ \xi_j^y = (y_{j-1} + y_j)/2, \ j = 1, \dots, N_y, \ \xi_{N_y+1}^y = y_R \right\}$$
(2.9)

to derive the so-called QSC-L1 scheme

$$\delta_{\tau} \boldsymbol{\theta}_{x} \boldsymbol{\theta}_{y} c_{i,j}^{n} + \lambda \delta_{\tau}^{1-\alpha_{n}} \boldsymbol{\theta}_{x} \boldsymbol{\theta}_{y} c_{i,j}^{n}$$

$$= d_{1} \boldsymbol{\eta}_{x} \boldsymbol{\theta}_{y} c_{i,j}^{n} + d_{2} \boldsymbol{\theta}_{x} \boldsymbol{\eta}_{y} c_{i,j}^{n} + f_{i,j}^{n}, \quad (i,j) \in \omega,$$
(2.10a)

$$\theta_x \theta_y c_{i,j}^n = \varphi_{i,j}^n,$$
 $(i,j) \in \partial \omega,$ (2.10b)

$$\theta_x \theta_y c_{i,j}^0 = u_{i,j}^o,$$
 $(i,j) \in \bar{\omega}$ (2.10c)

for $1 \le n \le N_t$. Here, $v_{i,j}^n = v(\xi_i^x, \xi_j^y, t_n)$ for $v = f, \varphi, u^o$, and the operators θ_x and η_x are defined by

$$\boldsymbol{\theta}_{x}c_{i,j}^{n} := \frac{1}{8} \begin{cases} 4c_{0,j}^{n} + 4c_{1,j}^{n}, & i = 0, \\ c_{i-1,j}^{n} + 6c_{i,j}^{n} + c_{i+1,j}^{n}, & i = 1, 2, \dots, N_{x}, \\ 4c_{N_{x},j}^{n} + 4c_{N_{x}+1,j}^{n}, & i = N_{x} + 1, \end{cases}$$
(2.11)

$$\eta_x c_{i,j}^n := \frac{1}{\Delta x^2} \left(c_{i-1,j}^n - 2c_{i,j}^n + c_{i+1,j}^n \right), \quad i = 1, 2, \dots, N_x.$$
(2.12)

Likewise, the operators θ_y and η_y can also be defined.

2.2. The ADI-QSC-L1 approximation

In this subsection, we consider an ADI approach for the approximation of the QSC-L1 method, in which the computational cost can be further reduced for large-scale modeling and simulations of (2.1).

Denote

$$s_n := \frac{1}{\tau} + \frac{\lambda b_n^{(n)}}{\Gamma(1 + \alpha_n)} = \mathcal{O}(\tau^{-1}).$$

Then, the QSC-L1 scheme (2.10a) can be rewritten as

$$\left[\boldsymbol{\theta}_{x}\boldsymbol{\theta}_{y} - \frac{d_{1}}{s_{n}}\boldsymbol{\eta}_{x}\boldsymbol{\theta}_{y} - \frac{d_{2}}{s_{n}}\boldsymbol{\theta}_{x}\boldsymbol{\eta}_{y}\right]c_{i,j}^{n} = F_{i,j}^{n}, \quad (i,j) \in \omega,$$
(2.13)

where

$$F_{i,j}^n := \frac{1}{s_n \tau} \theta_x \theta_y c_{i,j}^{n-1} + \frac{\lambda}{s_n \Gamma(1+\alpha_n)} \left[\sum_{k=1}^{n-1} \left(b_{k+1}^{(n)} - b_k^{(n)} \right) \theta_x \theta_y c_{i,j}^k + b_1^{(n)} \theta_x \theta_y c_{i,j}^0 \right] + \frac{1}{s_n} f_{i,j}^n.$$

Thus, an ADI approach, named ADI-QSC-L1, for approximation of model (2.1) from t_{n-1} to t_n can be proposed as follows:

Step 1. For each $j=1,2,\ldots,N_y$, solve a series of (N_x+2) -by- (N_x+2) linear algebra systems along x-direction

$$\begin{cases}
\theta_{x}c_{0,j}^{*} = \left(\theta_{y} - \frac{d_{2}}{s_{n}}\eta_{y}\right)\theta_{x}c_{0,j}^{n}, \\
\left(\theta_{x} - \frac{d_{1}}{s_{n}}\eta_{x}\right)c_{i,j}^{*} = \frac{d_{1}d_{2}}{s_{n}^{2}}\eta_{x}\eta_{y}c_{i,j}^{n-1} + F_{i,j}^{n}, \quad i = 1, 2, \dots, N_{x}, \\
\theta_{x}c_{N_{x}+1,j}^{*} = \left(\theta_{y} - \frac{d_{2}}{s_{n}}\eta_{y}\right)\theta_{x}c_{N_{x}+1,j}^{n},
\end{cases}$$
(2.14)

where $\{\theta_x c_{0,j}^n\}$ and $\{\theta_x c_{N_x+1,j}^n\}$ on the right-hand side of (2.14) are respectively given by solving (2.10b) at the left and right boundaries via

$$\theta_y(\theta_x c_{0,j}^n) = \varphi_{0,j}^n, \quad \theta_y(\theta_x c_{N_x+1,j}^n) = \varphi_{N_x+1,j}^n, \quad j = 0, 1, \dots, N_y + 1.$$
 (2.15)

Step 2. For each $i = 1, 2, ..., N_x$, solve a series of $(N_y + 2)$ -by- $(N_y + 2)$ linear algebra systems along y-direction

$$\left(\boldsymbol{\theta}_{y} - \frac{d_{2}}{s_{n}} \boldsymbol{\eta}_{y}\right) c_{i,j}^{n} = c_{i,j}^{*}, \quad j = 1, 2, \dots, N_{y}$$
 (2.16)

with boundary equations $\theta_y c_{i,0}^n$ and $\theta_y c_{i,N_y+1}^n$ determined by (2.10b) at the bottom and top boundaries that

$$\theta_x(\theta_y c_{i,0}^n) = \varphi_{i,0}^n, \quad \theta_x(\theta_y c_{i,N_y+1}^n) = \varphi_{i,N_y+1}^n, \quad i = 0, 1, \dots, N_x + 1.$$
 (2.17)

Finally, using the data $\{\theta_x c_{0,j}^n\}$ and $\{\theta_x c_{N_x+1,j}^n\}$ determined by (2.15), the left and right boundary values $\{c_{0,j}^n\}$ and $\{c_{N_x+1,j}^n\}$ are given by

$$c_{0,j}^n = 2\boldsymbol{\theta}_x c_{0,j}^n - c_{1,j}^n, \quad c_{N_x+1,j}^n = 2\boldsymbol{\theta}_x c_{N_x+1,j}^n - c_{N_x,j}^n, \quad j = 0, 1, \dots, N_y + 1,$$
 (2.18)

where $\{c_{1,i}^n\}$ and $\{c_{N_{n,i}}^n\}$ are obtained by linear systems (2.16)-(2.17).

Remark 2.1. For the first step of the aforementioned ADI-QSC-L1 scheme, we firstly have to solve two linear tri-diagonal systems (2.15) with scale (N_y+2) -by- (N_y+2) , to provide all the boundary values $\{\theta_x c_{0,j}^n\}$ and $\{\theta_x c_{N_x+1,j}^n\}$ for (2.14). Secondly, we have to solve two linear tri-diagonal systems (2.17) with scale (N_x+2) -by- (N_x+2) , to provide the boundary equations $\{\theta_y c_{i,0}^n\}$ and $\{\theta_y c_{i,N_y+1}^n\}$ for (2.16) in the second step.

Remark 2.2. We can see that, each system in (2.14) and (2.16) is linear, tri-diagonal, and only along one space direction, which can be solved efficiently using Thomas algorithm in $\mathcal{O}(N_x)$ or $\mathcal{O}(N_y)$ flops per time step. Thus, the computational cost is dramatically reduced compared with the QSC-L1 scheme (2.10). However, the calculation of the right-hand side of (2.13) involves the tridiagonal-matrix-vector multiplications of all the history time levels, which corresponds to $\mathcal{O}(nN_xN_y)$ operations. Thus, the

total computational complexity for the ADI-QSC-L1 scheme (2.14)-(2.18) is of order $\mathcal{O}(N_t^2N_xN_y)$, which is still computationally cost for long-term or small time stepsize modeling. Besides, the memory requirement is $\mathcal{O}(N_tN_xN_y)$ due to the nonlocal property of the time-fractional derivative. Therefore, an efficient solver is further required for the ADI-QSC-L1 method, and this shall be discussed in Section 4.

Remark 2.3. Note that the ADI-QSC-L1 scheme (2.14)-(2.18) is equivalent to

$$\begin{cases}
\left(\boldsymbol{\theta}_{x} - \frac{d_{1}}{s_{n}}\boldsymbol{\eta}_{x}\right) \left(\boldsymbol{\theta}_{y} - \frac{d_{2}}{s_{n}}\boldsymbol{\eta}_{y}\right) c_{i,j}^{n} = \frac{d_{1}d_{2}}{s_{n}^{2}}\boldsymbol{\eta}_{x}\boldsymbol{\eta}_{y}c_{i,j}^{n-1} + F_{i,j}^{n}, & (i,j) \in \omega, \\
\boldsymbol{\theta}_{x}\boldsymbol{\theta}_{y}c_{i,j}^{n} = \varphi_{i,j}^{n}, & (i,j) \in \partial\omega, \\
\boldsymbol{\theta}_{x}\boldsymbol{\theta}_{y}c_{i,j}^{0} = u_{i,j}^{o}, & (i,j) \in \bar{\omega}
\end{cases}$$

$$(2.19)$$

for $n = 1, ..., N_t$. In fact, compared with the direct QSC-L1 discretization (2.13), the ADI-QSC-L1 scheme (2.19) can be viewed as adding a high-order perturbation term

$$r_{3,n} := \frac{d_1 d_2}{s_n^2} \eta_x \eta_y (c_{i,j}^n - c_{i,j}^{n-1}) = \mathcal{O}(\tau^3)$$

into (2.13). Thus, the proposed ADI-QSC-L1 scheme (2.14)-(2.18) is actually a D'Yako-nov type ADI scheme.

3. Analysis of the ADI-QSC-L1 scheme

In this section, we shall analyze the ADI-QSC-L1 scheme (2.14)-(2.18) via the equivalent form (2.19) with respect to discrete L_2 norm.

3.1. Stability of the ADI-QSC-L1 scheme

We define

$$\mathcal{V}_h = \left\{ \boldsymbol{v} = (v_{i,j}) \in \mathbb{R}^{(N_x + 2) \times (N_y + 2)} : (i,j) \in \bar{\omega} \right\},
\mathcal{V}_h^0 = \left\{ \boldsymbol{v} \in \mathcal{V}_h : \boldsymbol{\theta}_x \boldsymbol{\theta}_y v_{i,\ell} = \boldsymbol{\theta}_x \boldsymbol{\theta}_y v_{\kappa,j} = 0, \ \kappa = 0, N_x + 1, \ \ell = 0, N_y + 1, \ (i,j) \in \bar{\omega} \right\}.$$

For any $w, v \in \mathcal{V}_h^0$, define the discrete inner products and norms

$$(\boldsymbol{w}, \boldsymbol{v}) := \Delta x \Delta y \sum_{i=1}^{N_x} \sum_{j=1}^{N_y} w_{i,j} \ v_{i,j}, \qquad \qquad \|\boldsymbol{v}\|^2 := (\boldsymbol{v}, \boldsymbol{v}),$$

$$\langle \boldsymbol{\delta}_x \boldsymbol{w}, \boldsymbol{\delta}_x \boldsymbol{v} \rangle_x := \Delta x \Delta y \sum_{i=1}^{N_x+1} \sum_{j=1}^{N_y} (\boldsymbol{\delta}_x w_{i,j}) (\boldsymbol{\delta}_x v_{i,j}), \quad \|\boldsymbol{\delta}_x \boldsymbol{v}\|_x^2 := \langle \boldsymbol{\delta}_x \boldsymbol{v}, \boldsymbol{\delta}_x \boldsymbol{v} \rangle_x,$$

where $\delta_x v_{i,j} = (v_{i,j} - v_{i-1,j})/\Delta x$, and similarly the discrete inner product $\langle \delta_y \boldsymbol{w}, \delta_y \boldsymbol{v} \rangle_y$ and norm $\|\delta_y \boldsymbol{v}\|_y$ can also be defined. We further define

$$\langle \boldsymbol{\delta}_{x} \boldsymbol{\delta}_{y} \boldsymbol{w}, \boldsymbol{\delta}_{x} \boldsymbol{\delta}_{y} \boldsymbol{v} \rangle_{xy} := \Delta x \Delta y \sum_{i=1}^{N_{x}+1} \sum_{j=1}^{N_{y}+1} (\boldsymbol{\delta}_{x} \boldsymbol{\delta}_{y} w_{i,j}) (\boldsymbol{\delta}_{x} \boldsymbol{\delta}_{y} v_{i,j}),$$

$$\|\boldsymbol{\delta}_{x} \boldsymbol{\delta}_{y} \boldsymbol{v}\|_{xy}^{2} := \langle \boldsymbol{\delta}_{x} \boldsymbol{\delta}_{y} \boldsymbol{v}, \boldsymbol{\delta}_{x} \boldsymbol{\delta}_{y} \boldsymbol{v} \rangle_{xy}.$$

The following lemmas play important roles in the stability analysis of the ADI-QSC-L1 scheme.

Lemma 3.1. For any $v \in \mathcal{V}_h^0$, we have

$$egin{aligned} (oldsymbol{\eta}_xoldsymbol{ heta}_yoldsymbol{v},oldsymbol{ heta}_xoldsymbol{ heta}_yoldsymbol{v}, \delta_xoldsymbol{ heta}_xoldsymbol{ heta}_yoldsymbol{v}_x,\ (oldsymbol{\eta}_yoldsymbol{ heta}_xoldsymbol{v},oldsymbol{ heta}_yoldsymbol{ heta}_xoldsymbol{v},\delta_yoldsymbol{ heta}_yoldsymbol{v},\delta_yoldsymbol{ heta}_yoldsymbol{v},\delta_yoldsymbol{ heta}_yoldsymbol{v},\delta_yoldsymbol{ heta}_yoldsymbol{v},\delta_yoldsymbol{ heta}_yoldsymbol{v},\delta_yoldsymbol{v}_yoldsymbol{v},\delta_yoldsymbol{ heta}_yoldsymbol{v}_yoldsymbol{v},\delta_yoldsymbol{ heta}_yoldsymbol{v}_yoldsymbol{v},\delta_yoldsymbol{ heta}_yoldsymbol{v}_yoldsymbol{v},\delta_yoldsymbol{v}_yoldsymbol{v}_yoldsymbol{v},\delta_yoldsymbol{v}_yoldsymbol{v}_yoldsymbol{v},\delta_yoldsymbol{v}_yoldsymbol{v}_yoldsymbol{v}_yoldsymbol{v},\delta_yoldsymbol{v}$$

Proof. We only prove the first conclusion, as the second one is a similar result along the y-direction. According to the definitions of the operators η_x and θ_x , we have

$$(\boldsymbol{\eta}_x \boldsymbol{\theta}_y \boldsymbol{v}, \boldsymbol{\theta}_x \boldsymbol{\theta}_y \boldsymbol{v}) = \Delta y \sum_{i=1}^{N_x} \sum_{i=1}^{N_y} (\boldsymbol{\delta}_x \boldsymbol{\theta}_y v_{i+1,j} - \boldsymbol{\delta}_x \boldsymbol{\theta}_y v_{i,j}) (\boldsymbol{\theta}_x \boldsymbol{\theta}_y v_{i,j}).$$

Noting that

$$\theta_x \theta_y v_{0,j} = \theta_x \theta_y v_{N_x+1,j} = 0,$$

and using summation by parts, we get

$$(\boldsymbol{\eta}_x\boldsymbol{\theta}_y\boldsymbol{v},\boldsymbol{\theta}_x\boldsymbol{\theta}_y\boldsymbol{v}) = -\Delta x\Delta y\sum_{i=1}^{N_x+1}\sum_{j=1}^{N_y}(\boldsymbol{\delta}_x\boldsymbol{\theta}_yv_{i,j})(\boldsymbol{\delta}_x\boldsymbol{\theta}_x\boldsymbol{\theta}_yv_{i,j}) = -\langle \boldsymbol{\delta}_x\boldsymbol{\theta}_y\boldsymbol{v},\,\boldsymbol{\delta}_x\boldsymbol{\theta}_x\boldsymbol{\theta}_y\boldsymbol{v}\rangle_x.$$

This completes the proof.

Lemma 3.2. For any $v \in \mathcal{V}_h^0$, we have

$$egin{aligned} \langle oldsymbol{\delta}_x oldsymbol{ heta}_x oldsymbol{ heta}_y oldsymbol{v} , oldsymbol{\delta}_x oldsymbol{ heta}_y oldsymbol{v}
angle_x \geq rac{1}{4} \|oldsymbol{\delta}_x oldsymbol{ heta}_y oldsymbol{v} \|_x^2, \ \langle oldsymbol{\delta}_y oldsymbol{ heta}_x oldsymbol{ heta}_y oldsymbol{v}, oldsymbol{\delta}_y oldsymbol{ heta}_x oldsymbol{v}
angle_x \geq rac{1}{4} \|oldsymbol{\delta}_y oldsymbol{ heta}_x oldsymbol{v} \|_x^2, \ \langle oldsymbol{\delta}_y oldsymbol{ heta}_x oldsymbol{ heta}_y oldsymbol{v}, oldsymbol{\delta}_y oldsymbol{ heta}_x oldsymbol{v} \|_x^2, \ \langle oldsymbol{\delta}_y oldsymbol{ heta}_x oldsymbol{ heta}_y oldsymbol{v}, oldsymbol{\delta}_y oldsymbol{ heta}_x oldsymbol{v} \|_x^2, \ \langle oldsymbol{\delta}_y oldsymbol{ heta}_x oldsymbol{ heta}_y oldsymbol{v} \|_x^2, \ \langle oldsymbol{\delta}_y oldsymbol{ heta}_x oldsymbol{ heta}_y oldsymbol{v} oldsymbol{v} \|_x^2, \ \langle oldsymbol{\delta}_y oldsymbol{ heta}_x oldsymbol{v} \|_x^2, \ \langle oldsymbol{\delta}_y oldsymbol{ heta}_x oldsymbol{v} \|_x^2, \ \langle oldsymbol{\delta}_y oldsymbol{\delta}_y oldsymbol{v} \|_x^2, \ \langle oldsymbol{\delta}_y oldsymbol{\delta}_y oldsymbol{\delta}_y oldsymbol{\delta}_y oldsymbol{\delta}_y oldsymbol{\delta}_y \end{picture}$$

Proof. We only prove the first conclusion, as the second one can be proved similarly. Following the homogeneous boundary conditions, we derive

$$\langle \boldsymbol{\delta}_{x} \boldsymbol{\theta}_{x} \boldsymbol{\theta}_{y} \boldsymbol{v}, \boldsymbol{\delta}_{x} \boldsymbol{\theta}_{y} \boldsymbol{v} \rangle_{x} = \Delta x \Delta y \sum_{i=1}^{N_{x}+1} \sum_{j=1}^{N_{y}} (\boldsymbol{\delta}_{x} \boldsymbol{\theta}_{y} v_{i,j}) (\boldsymbol{\delta}_{x} \boldsymbol{\theta}_{x} \boldsymbol{\theta}_{y} v_{i,j}) =: I + II + III, \quad (3.1)$$

where

$$I = \frac{\Delta x \Delta y}{8} \sum_{i=2}^{N_x} \sum_{j=1}^{N_y} (\boldsymbol{\delta}_x \boldsymbol{\theta}_y v_{i,j}) (\boldsymbol{\delta}_x \boldsymbol{\theta}_y v_{i-1,j} + 6 \boldsymbol{\delta}_x \boldsymbol{\theta}_y v_{i,j} + \boldsymbol{\delta}_x \boldsymbol{\theta}_y v_{i+1,j}),$$

$$II = \frac{\Delta y}{8} \sum_{j=1}^{N_y} (\boldsymbol{\delta}_x \boldsymbol{\theta}_y v_{1,j}) (\boldsymbol{\theta}_y v_{2,j} + 2\boldsymbol{\theta}_y v_{1,j} - 3\boldsymbol{\theta}_y v_{0,j}),$$

$$III = \frac{\Delta y}{8} \sum_{j=1}^{N_y} (\boldsymbol{\delta}_x \boldsymbol{\theta}_y v_{N_x+1,j}) (3\boldsymbol{\theta}_y v_{N_x+1,j} - 2\boldsymbol{\theta}_y v_{N_x,j} - \boldsymbol{\theta}_y v_{N_x-1,j}).$$

First, using $ab \ge (-1/2)(a^2 + b^2)$ we see

$$I \geq \frac{\Delta x \Delta y}{8} \sum_{i=2}^{N_x} \sum_{j=1}^{N_y} \left[-\frac{1}{2} (\boldsymbol{\delta}_x \boldsymbol{\theta}_y v_{i-1,j})^2 + 5(\boldsymbol{\delta}_x \boldsymbol{\theta}_y v_{i,j})^2 - \frac{1}{2} (\boldsymbol{\delta}_x \boldsymbol{\theta}_y v_{i+1,j})^2 \right].$$

Second, for the homogeneous boundary conditions $\theta_x \theta_y v_{0,j} = 0$ for $j = 1, \dots, N_y$, we have

$$\theta_y v_{1,j} = -\theta_y v_{0,j},\tag{3.2}$$

which leads to

$$II = \frac{\Delta x \Delta y}{8} \sum_{j=1}^{N_y} (\delta_x \theta_y v_{1,j}) \left[\delta_x \theta_y v_{2,j} + 3 \delta_x \theta_y v_{1,j} \right]$$
$$\geq \frac{\Delta x \Delta y}{8} \sum_{j=1}^{N_y} \left[\frac{5}{2} (\delta_x \theta_y v_{1,j})^2 - \frac{1}{2} (\delta_x \theta_y v_{2,j})^2 \right],$$

and similarly, because of $\theta_x\theta_yv_{N_x+1,j}=0$, the third term is bounded below as

$$III \geq \frac{\Delta x \Delta y}{8} \sum_{i=1}^{N_y} \left[\frac{5}{2} (\boldsymbol{\delta}_x \boldsymbol{\theta}_y v_{N_x+1,j})^2 - \frac{1}{2} (\boldsymbol{\delta}_x \boldsymbol{\theta}_y v_{N_x,j})^2 \right].$$

Thus, inserting the above estimates into (3.1), we immediately get

$$\langle \boldsymbol{\delta}_{x} \boldsymbol{\theta}_{x} \boldsymbol{\theta}_{y} \boldsymbol{v}, \boldsymbol{\delta}_{x} \boldsymbol{\theta}_{y} \boldsymbol{v} \rangle_{x}$$

$$\geq \frac{\Delta x \Delta y}{8} \sum_{j=1}^{N_{y}} \left[2(\boldsymbol{\delta}_{x} \boldsymbol{\theta}_{y} v_{1,j})^{2} + 4 \sum_{i=2}^{N_{x}} (\boldsymbol{\delta}_{x} \boldsymbol{\theta}_{y} v_{i,j})^{2} + 2(\boldsymbol{\delta}_{x} \boldsymbol{\theta}_{y} v_{N_{x}+1,j})^{2} \right]$$

$$\geq \frac{1}{4} \|\boldsymbol{\delta}_{x} \boldsymbol{\theta}_{y} \boldsymbol{v}\|_{x}^{2},$$

which proves the first conclusion of Lemma 3.2.

Lemma 3.3. For any $v \in \mathcal{V}_h^0$, we have

$$\frac{1}{32} \|\boldsymbol{\delta}_x \boldsymbol{\delta}_y \boldsymbol{v}\|_{xy}^2 \le (\boldsymbol{\eta}_x \boldsymbol{\eta}_y \boldsymbol{v}, \boldsymbol{\theta}_x \boldsymbol{\theta}_y \boldsymbol{v}) \le \frac{23}{32} \|\boldsymbol{\delta}_x \boldsymbol{\delta}_y \boldsymbol{v}\|_{xy}^2.$$

Proof. Using summation by parts for the indices j and i, respectively, we have

$$(oldsymbol{\eta}_xoldsymbol{\eta}_yoldsymbol{v},oldsymbol{ heta}_xoldsymbol{ heta}_yoldsymbol{v},oldsymbol{\delta}_xoldsymbol{ heta}_xoldsymbol{ heta}_yoldsymbol{v},oldsymbol{\delta}_xoldsymbol{ heta}_yoldsymbol{v}
angle_{xy}$$

Then, according to the definition of inner product, we see

$$\langle \delta_{x}\delta_{y}v, \delta_{x}\delta_{y}\theta_{x}\theta_{y}v \rangle_{xy}$$

$$= \Delta x \Delta y \sum_{i=1}^{N_{x}+1} \sum_{j=1}^{N_{y}+1} (\theta_{x}\theta_{y}\delta_{x}\delta_{y}v_{i,j})(\delta_{x}\delta_{y}v_{i,j})$$

$$= \Delta x \Delta y \left[(\theta_{x}\theta_{y}\delta_{x}\delta_{y}v_{1,1})(\delta_{x}\delta_{y}v_{1,1}) + \sum_{j=2}^{N_{y}} (\theta_{x}\theta_{y}\delta_{x}\delta_{y}v_{1,j})(\delta_{x}\delta_{y}v_{1,j}) + (\theta_{x}\theta_{y}\delta_{x}\delta_{y}v_{1,N_{y}+1})(\delta_{x}\delta_{y}v_{1,N_{y}+1}) + \sum_{i=2}^{N_{x}} (\theta_{x}\theta_{y}\delta_{x}\delta_{y}v_{i,1})(\delta_{x}\delta_{y}v_{i,1}) + \sum_{i=2}^{N_{x}} \sum_{j=2}^{N_{y}} (\theta_{x}\theta_{y}\delta_{x}\delta_{y}v_{i,j})(\delta_{x}\delta_{y}v_{i,j}) + \sum_{i=2}^{N_{x}} (\theta_{x}\theta_{y}\delta_{x}\delta_{y}v_{i,N_{y}+1})(\delta_{x}\delta_{y}v_{i,N_{y}+1})$$

$$+ (\theta_{x}\theta_{y}\delta_{x}\delta_{y}v_{N_{x}+1,1})(\delta_{x}\delta_{y}v_{N_{x}+1,1}) + \sum_{j=2}^{N_{y}} (\theta_{x}\theta_{y}\delta_{x}\delta_{y}v_{N_{x}+1,j})(\delta_{x}\delta_{y}v_{N_{x}+1,j})$$

$$+ (\theta_{x}\theta_{y}\delta_{x}\delta_{y}v_{N_{x}+1,N_{y}+1})(\delta_{x}\delta_{y}v_{N_{x}+1,N_{y}+1}) \right] =: \sum_{i=1}^{9} \mathcal{P}_{i}. \tag{3.3}$$

For the term \mathcal{P}_1 in (3.3), since $\theta_x \theta_y v_{i,0} = 0$ for $i = 0, 1, \dots, N_x + 1$, we have

$$\boldsymbol{\theta}_x \boldsymbol{\theta}_y \boldsymbol{\delta}_x \boldsymbol{\delta}_y v_{1,1} = \frac{1}{\Delta x \Delta y} \boldsymbol{\theta}_x \boldsymbol{\theta}_y (v_{1,1} - v_{0,1} - v_{1,0} + v_{0,0}) = \frac{1}{\Delta x \Delta y} \boldsymbol{\theta}_x \boldsymbol{\theta}_y v_{1,1},$$

and thus by (3.2), we see

$$\mathcal{P}_{1} = (\boldsymbol{\delta}_{x}\boldsymbol{\delta}_{y}v_{1,1})(\boldsymbol{\theta}_{x}\boldsymbol{\theta}_{y}v_{1,1})$$

$$= \frac{1}{8}(\boldsymbol{\delta}_{x}\boldsymbol{\delta}_{y}v_{1,1})[\boldsymbol{\theta}_{y}v_{2,1} - \boldsymbol{\theta}_{y}v_{1,1} + 3(\boldsymbol{\theta}_{y}v_{1,1} - \boldsymbol{\theta}_{y}v_{0,1})]$$

$$= \frac{\Delta x}{8}(\boldsymbol{\delta}_{x}\boldsymbol{\delta}_{y}v_{1,1})[\boldsymbol{\delta}_{x}\boldsymbol{\theta}_{y}v_{2,1} + 3\boldsymbol{\delta}_{x}\boldsymbol{\theta}_{y}v_{1,1}]. \tag{3.4}$$

Furthermore, taking the same routine for the operator θ_y in (3.4), we can obtain

$$\mathcal{P}_1 = \frac{\Delta x \Delta y}{64} (\boldsymbol{\delta}_x \boldsymbol{\delta}_y v_{1,1}) [\boldsymbol{\delta}_x \boldsymbol{\delta}_y v_{2,2} + 3 \boldsymbol{\delta}_x \boldsymbol{\delta}_y v_{2,1} + 3 \boldsymbol{\delta}_x \boldsymbol{\delta}_y v_{1,2} + 9 \boldsymbol{\delta}_x \boldsymbol{\delta}_y v_{1,1}],$$

from which and using the inequality $ab \ge (-1/2)(a^2 + b^2)$, we have

$$\mathcal{P}_1 \ge \frac{\Delta x \Delta y}{128} \left[11 (\boldsymbol{\delta}_x \boldsymbol{\delta}_y v_{1,1})^2 - (\boldsymbol{\delta}_x \boldsymbol{\delta}_y v_{2,2})^2 - 3 (\boldsymbol{\delta}_x \boldsymbol{\delta}_y v_{2,1})^2 - 3 (\boldsymbol{\delta}_x \boldsymbol{\delta}_y v_{1,2})^2 \right].$$

Similarly, for the terms \mathcal{P}_3 , \mathcal{P}_7 and \mathcal{P}_9 we have

$$\mathcal{P}_{3} \geq \frac{\Delta x \Delta y}{128} \left[11(\delta_{x} \delta_{y} v_{1,N_{y}+1})^{2} - (\delta_{x} \delta_{y} v_{2,N_{y}})^{2} - 3(\delta_{x} \delta_{y} v_{2,N_{y}+1})^{2} - 3(\delta_{x} \delta_{y} v_{1,N_{y}})^{2} \right],$$

$$\mathcal{P}_{7} \geq \frac{\Delta x \Delta y}{128} \left[11(\delta_{x} \delta_{y} v_{N_{x}+1,1})^{2} - (\delta_{x} \delta_{y} v_{N_{x},2})^{2} - 3(\delta_{x} \delta_{y} v_{N_{x}+1,2})^{2} - 3(\delta_{x} \delta_{y} v_{N_{x},1})^{2} \right],$$

$$\mathcal{P}_{9} \geq \frac{\Delta x \Delta y}{128} \left[11(\delta_{x} \delta_{y} v_{N_{x}+1,N_{y}+1})^{2} - (\delta_{x} \delta_{y} v_{N_{x},N_{y}})^{2} - 3(\delta_{x} \delta_{y} v_{N_{x}+1,N_{y}})^{2} - 3(\delta_{x} \delta_{y} v_{N_{x}+1,N_{y}})^{2} - 3(\delta_{x} \delta_{y} v_{N_{x},N_{y}+1})^{2} \right].$$

For the term \mathcal{P}_2 , by the homogeneous boundary conditions, we have

$$\begin{split} \theta_x \theta_y \delta_x \delta_y v_{1,j} &= \frac{1}{\Delta x} \theta_x \theta_y \delta_y v_{1,j} \\ &= \frac{1}{8\Delta x} \delta_y \theta_y (v_{2,j} + 6v_{1,j} + v_{0,j}) \\ &= \frac{1}{8\Delta x} \delta_y \theta_y [v_{2,j} - v_{1,j} + 3(v_{1,j} - v_{0,j})] \\ &= \frac{1}{8} \delta_y \theta_y \delta_x (v_{2,j} + 3v_{1,j}) \\ &= \frac{1}{64} \delta_x \delta_y (v_{2,j-1} + 6v_{2,j} + v_{2,j+1} + 3v_{1,j-1} + 18v_{1,j} + 3v_{1,j+1}) \end{split}$$

for $j = 2, \ldots, N_y$. Then,

$$\mathcal{P}_{2} \ge \frac{\Delta x \Delta y}{128} \sum_{j=2}^{N_{y}} \left[22(\delta_{x} \delta_{y} v_{1,j})^{2} - 3(\delta_{x} \delta_{y} v_{1,j-1})^{2} - 3(\delta_{x} \delta_{y} v_{1,j+1})^{2} - (\delta_{x} \delta_{y} v_{2,j-1})^{2} - 6(\delta_{x} \delta_{y} v_{2,j})^{2} - (\delta_{x} \delta_{y} v_{2,j+1})^{2} \right].$$

Similarly, we have

$$\mathcal{P}_{4} \geq \frac{\Delta x \Delta y}{128} \sum_{i=2}^{N_{x}} \left[22(\delta_{x}\delta_{y}v_{i,1})^{2} - 3(\delta_{x}\delta_{y}v_{i-1,1})^{2} - 3(\delta_{x}\delta_{y}v_{i+1,1})^{2} - (\delta_{x}\delta_{y}v_{i-1,2})^{2} - 6(\delta_{x}\delta_{y}v_{i,2})^{2} - (\delta_{x}\delta_{y}v_{i+1,2})^{2} \right],$$

$$\mathcal{P}_{6} \geq \frac{\Delta x \Delta y}{128} \sum_{i=2}^{N_{x}} \left[22(\delta_{x}\delta_{y}v_{i,N_{y}+1})^{2} - 3(\delta_{x}\delta_{y}v_{i-1,N_{y}+1})^{2} - 3(\delta_{x}\delta_{y}v_{i+1,N_{y}+1})^{2} - (\delta_{x}\delta_{y}v_{i-1,N_{y}})^{2} - (\delta_{x}\delta_{y}v_{i+1,N_{y}})^{2} \right],$$

$$\mathcal{P}_{8} \geq \frac{\Delta x \Delta y}{128} \sum_{j=2}^{N_{y}} \left[22(\delta_{x}\delta_{y}v_{N_{x}+1,j})^{2} - 3(\delta_{x}\delta_{y}v_{N_{x}+1,j-1})^{2} - 3(\delta_{x}\delta_{y}v_{N_{x}+1,j+1})^{2} - 3(\delta_{x}\delta_{y}v_{N_{x},j-1})^{2} - 6(\delta_{x}\delta_{y}v_{N_{x},j})^{2} - (\delta_{x}\delta_{y}v_{N_{x},j+1})^{2} \right].$$

Finally, for the term \mathcal{P}_5 , we have for $i=2,\ldots,N_x$, $j=2,\ldots,N_y$,

$$\theta_x \theta_y \delta_x \delta_y v_{i,j} = \frac{1}{64} \delta_x \delta_y \left(v_{i-1,j-1} + 6v_{i,j-1} + v_{i+1,j-1} + 6v_{i-1,j} + 36v_{i,j} + 6v_{i+1,j} + v_{i-1,j+1} + 6v_{i,j+1} + v_{i+1,j+1} \right),$$

and thus

$$\mathcal{P}_{5} \geq \frac{\Delta x \Delta y}{128} \sum_{i=2}^{N_{x}} \sum_{j=2}^{N_{y}} \left[44(\boldsymbol{\delta}_{x} \boldsymbol{\delta}_{y} v_{i,j})^{2} - (\boldsymbol{\delta}_{x} \boldsymbol{\delta}_{y} v_{i-1,j-1})^{2} - 6(\boldsymbol{\delta}_{x} \boldsymbol{\delta}_{y} v_{i,j-1})^{2} - (\boldsymbol{\delta}_{x} \boldsymbol{\delta}_{y} v_{i+1,j-1})^{2} - 6(\boldsymbol{\delta}_{x} \boldsymbol{\delta}_{y} v_{i-1,j})^{2} - 6(\boldsymbol{\delta}_{x} \boldsymbol{\delta}_{y} v_{i+1,j})^{2} - (\boldsymbol{\delta}_{x} \boldsymbol{\delta}_{y} v_{i-1,j+1})^{2} - 6(\boldsymbol{\delta}_{x} \boldsymbol{\delta}_{y} v_{i,j+1})^{2} - (\boldsymbol{\delta}_{x} \boldsymbol{\delta}_{y} v_{i+1,j+1})^{2} \right].$$

Now, inserting the lower-bound estimates of $\mathcal{P}_1 - \mathcal{P}_9$ into (3.3), we have

$$\begin{split} &\langle \boldsymbol{\delta}_{x} \boldsymbol{\delta}_{y} \boldsymbol{v}, \boldsymbol{\delta}_{x} \boldsymbol{\delta}_{y} \boldsymbol{\theta}_{x} \boldsymbol{\theta}_{y} \boldsymbol{v} \rangle_{xy} \\ &\geq \frac{\Delta x \Delta y}{128} \left[8 \sum_{i=2}^{N_{x}} (\boldsymbol{\delta}_{x} \boldsymbol{\delta}_{y} v_{i,1})^{2} + 16 \sum_{i=2}^{N_{x}-1} (\boldsymbol{\delta}_{x} \boldsymbol{\delta}_{y} v_{i,2})^{2} + 16 \sum_{i=3}^{N_{x}} (\boldsymbol{\delta}_{x} \boldsymbol{\delta}_{y} v_{i,N_{y}})^{2} \right. \\ &\quad + 8 \sum_{i=2}^{N_{x}} (\boldsymbol{\delta}_{x} \boldsymbol{\delta}_{y} v_{i,N_{y}+1})^{2} + 8 \sum_{j=2}^{N_{y}} (\boldsymbol{\delta}_{x} \boldsymbol{\delta}_{y} v_{1,j})^{2} + 16 \sum_{j=3}^{N_{y}} (\boldsymbol{\delta}_{x} \boldsymbol{\delta}_{y} v_{2,j})^{2} \\ &\quad + 16 \sum_{j=2}^{N_{y}-1} (\boldsymbol{\delta}_{x} \boldsymbol{\delta}_{y} v_{N_{x},j})^{2} + 8 \sum_{j=2}^{N_{y}} (\boldsymbol{\delta}_{x} \boldsymbol{\delta}_{y} v_{N_{x}+1,j})^{2} + 4 (\boldsymbol{\delta}_{x} \boldsymbol{\delta}_{y} v_{1,1})^{2} \\ &\quad + 4 (\boldsymbol{\delta}_{x} \boldsymbol{\delta}_{y} v_{N_{x}+1,1})^{2} + 4 (\boldsymbol{\delta}_{x} \boldsymbol{\delta}_{y} v_{N_{x}+1,N_{y}+1})^{2} + 4 (\boldsymbol{\delta}_{x} \boldsymbol{\delta}_{y} v_{1,N_{y}+1})^{2} \\ &\quad + 36 \sum_{i=3}^{N_{x}-1} \sum_{j=3}^{N_{y}-1} (\boldsymbol{\delta}_{x} \boldsymbol{\delta}_{y} v_{i,j})^{2} \right] \\ &\geq \frac{1}{22} \|\boldsymbol{\delta}_{x} \boldsymbol{\delta}_{y} \boldsymbol{v}\|_{xy}^{2}, \end{split}$$

which proves the left part of the conclusion.

On the other hand, by a similar routine we can derive the upper-bound of \mathcal{P}_i $(i = 1, \dots, 9)$, and therefore

$$\langle \boldsymbol{\delta}_{x} \boldsymbol{\delta}_{y} \boldsymbol{v}, \boldsymbol{\delta}_{x} \boldsymbol{\delta}_{y} \boldsymbol{\theta}_{x} \boldsymbol{\theta}_{y} \boldsymbol{v} \rangle_{xy}$$

$$\leq \frac{\Delta x \Delta y}{128} \left[46 \sum_{i=2}^{N_{x}} (\boldsymbol{\delta}_{x} \boldsymbol{\delta}_{y} v_{i,1})^{2} + 46 \sum_{i=2}^{N_{x}} (\boldsymbol{\delta}_{x} \boldsymbol{\delta}_{y} v_{i,N_{y}+1})^{2} + 46 \sum_{j=2}^{N_{y}} (\boldsymbol{\delta}_{x} \boldsymbol{\delta}_{y} v_{1,j})^{2} + 46 \sum_{j=2}^{N_{y}} (\boldsymbol{\delta}_{x} \boldsymbol{\delta}_{y} v_{N_{x}+1,j})^{2} + 23 (\boldsymbol{\delta}_{x} \boldsymbol{\delta}_{y} v_{1,1})^{2} + 23 (\boldsymbol{\delta}_{x} \boldsymbol{\delta}_{y} v_{N_{x}+1,1})^{2} \right]$$

$$+23(\boldsymbol{\delta}_{x}\boldsymbol{\delta}_{y}v_{1,N_{y}+1})^{2}+23(\boldsymbol{\delta}_{x}\boldsymbol{\delta}_{y}v_{N_{x}+1,N_{y}+1})^{2}+92\sum_{i=2}^{N_{x}}\sum_{j=2}^{N_{y}}(\boldsymbol{\delta}_{x}\boldsymbol{\delta}_{y}v_{i,j})^{2}\right]$$

$$\leq \frac{23}{32}\|\boldsymbol{\delta}_{x}\boldsymbol{\delta}_{y}\boldsymbol{v}\|_{xy}^{2},$$

which proves the right part of the conclusion.

With the help of the above preliminary lemmas, the stability of the ADI-QSC-L1 scheme is included in the following theorem.

Theorem 3.1 (Stability). Let $\{c_{i,j}^n | (i,j) \in \bar{\omega}, 0 \le n \le N_t\}$ be the solution of the ADI-QSC-L1 scheme (2.19). Then, we have

$$\|\boldsymbol{\theta}_x\boldsymbol{\theta}_y\boldsymbol{c}^n\|^2 \leq Q\left[\|\boldsymbol{\theta}_x\boldsymbol{\theta}_y\boldsymbol{c}^0\|^2 + \tau^2d_1d_2\|\boldsymbol{\delta}_x\boldsymbol{\delta}_y\boldsymbol{c}^0\|_{xy}^2 + \tau\sum_{k=1}^n\|\boldsymbol{f}^k\|^2\right],$$

where Q is a positive constant.

Proof. We first rewrite (2.19) into the following equivalent form:

$$\left(s_n \boldsymbol{\theta}_x \boldsymbol{\theta}_y - d_1 \boldsymbol{\eta}_x \boldsymbol{\theta}_y - d_2 \boldsymbol{\theta}_x \boldsymbol{\eta}_y + \frac{d_1 d_2}{s_n} \boldsymbol{\eta}_x \boldsymbol{\eta}_y\right) c_{i,j}^n = \frac{d_1 d_2}{s_n} \boldsymbol{\eta}_x \boldsymbol{\eta}_y c_{i,j}^{n-1} + s_n F_{i,j}^n.$$
(3.5)

Then, multiplying both sides of (3.5) by $\Delta x \Delta y \theta_x \theta_y c_{i,j}^n$, and summing up for i from 1 to N_x and for j from 1 to N_y , we obtain

$$s_{n} \|\boldsymbol{\theta}_{x}\boldsymbol{\theta}_{y}\boldsymbol{c}^{n}\|^{2} + \frac{d_{1}d_{2}}{s_{n}} (\boldsymbol{\eta}_{x}\boldsymbol{\eta}_{y}\boldsymbol{c}^{n}, \boldsymbol{\theta}_{x}\boldsymbol{\theta}_{y}\boldsymbol{c}^{n})$$

$$= \frac{1}{\tau} \left(\boldsymbol{\theta}_{x}\boldsymbol{\theta}_{y}\boldsymbol{c}^{n-1}, \boldsymbol{\theta}_{x}\boldsymbol{\theta}_{y}\boldsymbol{c}^{n}\right) + \frac{\lambda}{\Gamma(1+\alpha_{n})} \sum_{k=1}^{n-1} \left(b_{k+1}^{(n)} - b_{k}^{(n)}\right) \left(\boldsymbol{\theta}_{x}\boldsymbol{\theta}_{y}\boldsymbol{c}^{k}, \boldsymbol{\theta}_{x}\boldsymbol{\theta}_{y}\boldsymbol{c}^{n}\right)$$

$$+ \frac{\lambda b_{1}^{(n)}}{\Gamma(1+\alpha_{n})} \left(\boldsymbol{\theta}_{x}\boldsymbol{\theta}_{y}\boldsymbol{c}^{0}, \boldsymbol{\theta}_{x}\boldsymbol{\theta}_{y}\boldsymbol{c}^{n}\right) + d_{1} \left(\boldsymbol{\eta}_{x}\boldsymbol{\theta}_{y}\boldsymbol{c}^{n}, \boldsymbol{\theta}_{x}\boldsymbol{\theta}_{y}\boldsymbol{c}^{n}\right) + d_{2} \left(\boldsymbol{\theta}_{x}\boldsymbol{\eta}_{y}\boldsymbol{c}^{n}, \boldsymbol{\theta}_{x}\boldsymbol{\theta}_{y}\boldsymbol{c}^{n}\right)$$

$$+ \frac{d_{1}d_{2}}{s_{n}} \left(\boldsymbol{\eta}_{x}\boldsymbol{\eta}_{y}\boldsymbol{c}^{n-1}, \boldsymbol{\theta}_{x}\boldsymbol{\theta}_{y}\boldsymbol{c}^{n}\right) + (\boldsymbol{f}^{n}, \boldsymbol{\theta}_{x}\boldsymbol{\theta}_{y}\boldsymbol{c}^{n}). \tag{3.6}$$

For the fourth and fifth terms on the right-hand side of (3.6), by using Lemmas 3.1-3.2, we have

$$d_{1} (\boldsymbol{\eta}_{x}\boldsymbol{\theta}_{y}\boldsymbol{c}^{n}, \boldsymbol{\theta}_{x}\boldsymbol{\theta}_{y}\boldsymbol{c}^{n}) + d_{2} (\boldsymbol{\theta}_{x}\boldsymbol{\eta}_{y}\boldsymbol{c}^{n}, \boldsymbol{\theta}_{x}\boldsymbol{\theta}_{y}\boldsymbol{c}^{n})$$

$$= -d_{1} \langle \boldsymbol{\delta}_{x}\boldsymbol{\theta}_{x}\boldsymbol{\theta}_{y}\boldsymbol{c}^{n}, \boldsymbol{\delta}_{x}\boldsymbol{\theta}_{y}\boldsymbol{c}^{n} \rangle_{x} - d_{2} \langle \boldsymbol{\delta}_{y}\boldsymbol{\theta}_{x}\boldsymbol{\theta}_{y}\boldsymbol{c}^{n}, \boldsymbol{\delta}_{y}\boldsymbol{\theta}_{x}\boldsymbol{c}^{n} \rangle_{y}$$

$$\leq -\frac{d_{1}}{4} \|\boldsymbol{\delta}_{x}\boldsymbol{\theta}_{y}\boldsymbol{c}^{n}\|_{x}^{2} - \frac{d_{2}}{4} \|\boldsymbol{\delta}_{y}\boldsymbol{\theta}_{x}\boldsymbol{c}^{n}\|_{y}^{2} \leq 0.$$
(3.7)

Notice that (2.11) implies that θ_x is a symmetric positive definite operator. Then, there exists an operator ϑ_x satisfying $\theta_x = \vartheta_x^2$, and similarly, there is also an operator ϑ_y satisfying $\theta_y = \vartheta_y^2$. Similar to the proof of Lemma 3.1, we have

$$(\eta_x \eta_y c^{n-1}, \theta_x \theta_y c^n) = \langle \delta_x \delta_y \vartheta_x \vartheta_y c^{n-1}, \delta_x \delta_y \vartheta_x \vartheta_y c^n \rangle_{xy}. \tag{3.8}$$

Inserting (3.7)-(3.8) into (3.6), and by Cauchy-Schwarz inequality we get

$$\begin{split} & s_{n} \|\boldsymbol{\theta}_{x}\boldsymbol{\theta}_{y}\boldsymbol{c}^{n}\|^{2} + \frac{d_{1}d_{2}}{s_{n}} \|\boldsymbol{\delta}_{x}\boldsymbol{\delta}_{y}\boldsymbol{\vartheta}_{x}\boldsymbol{\vartheta}_{y}\boldsymbol{c}^{n}\|_{xy}^{2} \\ & \leq \frac{1}{2\tau} \left[\|\boldsymbol{\theta}_{x}\boldsymbol{\theta}_{y}\boldsymbol{c}^{n-1}\|^{2} + \|\boldsymbol{\theta}_{x}\boldsymbol{\theta}_{y}\boldsymbol{c}^{n}\|^{2} \right] \\ & \quad + \frac{\lambda}{2\Gamma(1+\alpha_{n})} \sum_{k=1}^{n-1} \left(b_{k+1}^{(n)} - b_{k}^{(n)} \right) \left[\|\boldsymbol{\theta}_{x}\boldsymbol{\theta}_{y}\boldsymbol{c}^{k}\|^{2} + \|\boldsymbol{\theta}_{x}\boldsymbol{\theta}_{y}\boldsymbol{c}^{n}\|^{2} \right] \\ & \quad + \frac{\lambda b_{1}^{(n)}}{2\Gamma(1+\alpha_{n})} \left[\|\boldsymbol{\theta}_{x}\boldsymbol{\theta}_{y}\boldsymbol{c}^{0}\|^{2} + \|\boldsymbol{\theta}_{x}\boldsymbol{\theta}_{y}\boldsymbol{c}^{n}\|^{2} \right] + \frac{1}{2} \left[\|\boldsymbol{f}^{n}\|^{2} + \|\boldsymbol{\theta}_{x}\boldsymbol{\theta}_{y}\boldsymbol{c}^{n}\|^{2} \right] \\ & \quad + \frac{d_{1}d_{2}}{2s_{n}} \left[\|\boldsymbol{\delta}_{x}\boldsymbol{\delta}_{y}\boldsymbol{\vartheta}_{x}\boldsymbol{\vartheta}_{y}\boldsymbol{c}^{n-1}\|_{xy}^{2} + \|\boldsymbol{\delta}_{x}\boldsymbol{\delta}_{y}\boldsymbol{\vartheta}_{x}\boldsymbol{\vartheta}_{y}\boldsymbol{c}^{n}\|_{xy}^{2} \right] \\ & \quad \leq \frac{1}{2\tau} \|\boldsymbol{\theta}_{x}\boldsymbol{\theta}_{y}\boldsymbol{c}^{n-1}\|^{2} + \frac{\lambda}{2\Gamma(1+\alpha_{n})} \sum_{k=1}^{n-1} (b_{k+1}^{(n)} - b_{k}^{(n)}) \|\boldsymbol{\theta}_{x}\boldsymbol{\theta}_{y}\boldsymbol{c}^{k}\|^{2} \\ & \quad + \frac{\lambda b_{1}^{(n)}}{2\Gamma(1+\alpha_{n})} \|\boldsymbol{\theta}_{x}\boldsymbol{\theta}_{y}\boldsymbol{c}^{0}\|^{2} + \frac{d_{1}d_{2}}{2s_{n}} \|\boldsymbol{\delta}_{x}\boldsymbol{\delta}_{y}\boldsymbol{\vartheta}_{x}\boldsymbol{\vartheta}_{y}\boldsymbol{c}^{n-1}\|_{xy}^{2} \\ & \quad + \frac{1}{2} \|\boldsymbol{f}^{n}\|^{2} + \frac{s_{n}+1}{2} \|\boldsymbol{\theta}_{x}\boldsymbol{\theta}_{y}\boldsymbol{c}^{n}\|^{2} + \frac{d_{1}d_{2}}{2s_{n}} \|\boldsymbol{\delta}_{x}\boldsymbol{\delta}_{y}\boldsymbol{\vartheta}_{x}\boldsymbol{\vartheta}_{y}\boldsymbol{c}^{n}\|_{xy}^{2}, \end{split}$$

where the monotonicity of the coefficients $\{b_k^{(n)}\}$ in (2.5) has been used. We further have

$$\tau \mu_{n} \|\boldsymbol{\theta}_{x} \boldsymbol{\theta}_{y} \boldsymbol{c}^{n}\|^{2} + \tau \frac{d_{1} d_{2}}{s_{n}} \|\boldsymbol{\delta}_{x} \boldsymbol{\delta}_{y} \boldsymbol{\vartheta}_{x} \boldsymbol{\vartheta}_{y} \boldsymbol{c}^{n}\|_{xy}^{2}$$

$$\leq \|\boldsymbol{\theta}_{x} \boldsymbol{\theta}_{y} \boldsymbol{c}^{n-1}\|^{2} + \frac{\lambda \tau}{\Gamma(1+\alpha_{n})} \sum_{k=1}^{n-1} \left(b_{k+1}^{(n)} - b_{k}^{(n)}\right) \|\boldsymbol{\theta}_{x} \boldsymbol{\theta}_{y} \boldsymbol{c}^{k}\|^{2}$$

$$+ \frac{\lambda \tau b_{1}^{(n)}}{\Gamma(1+\alpha_{n})} \|\boldsymbol{\theta}_{x} \boldsymbol{\theta}_{y} \boldsymbol{c}^{0}\|^{2} + \tau \frac{d_{1} d_{2}}{s_{n}} \|\boldsymbol{\delta}_{x} \boldsymbol{\delta}_{y} \boldsymbol{\vartheta}_{x} \boldsymbol{\vartheta}_{y} \boldsymbol{c}^{n-1}\|_{xy}^{2} + \tau \|\boldsymbol{f}^{n}\|^{2}, \tag{3.9}$$

where, for τ sufficiently small, $\mu_n := s_n - 1 > 0$. Furthermore, note that $1/s_n < \tau \le 2\tau$, and thus for τ sufficiently small,

$$\frac{1}{\mu_n} < \tau \le 2\tau, \quad \frac{s_n}{\mu_n} = 1 + \frac{1}{\mu_n} \le 1 + 2\tau.$$
 (3.10)

We further denote

$$\sigma_m := \frac{1}{\tau} + \frac{\lambda (b_m^{(m)} - b_{m-1}^{(m)})}{\Gamma(1 + \alpha_m)} = \frac{1}{\tau} + \frac{\lambda (2 - 2^{\alpha_m}) \tau^{\alpha_m}}{\tau \Gamma(1 + \alpha_m)}.$$

Next, we start from (3.9) to prove the following induction result:

$$\|\boldsymbol{\theta}_{x}\boldsymbol{\theta}_{y}\boldsymbol{c}^{n}\|^{2} + \frac{d_{1}d_{2}}{s_{n}\mu_{n}}\|\boldsymbol{\delta}_{x}\boldsymbol{\delta}_{y}\boldsymbol{\vartheta}_{x}\boldsymbol{\vartheta}_{y}\boldsymbol{c}^{n}\|_{xy}^{2} \leq \Phi^{n}, \tag{3.11}$$

where

$$\Phi^{0} := \|\boldsymbol{\theta}_{x}\boldsymbol{\theta}_{y}\boldsymbol{c}^{0}\|^{2} + \tau^{2}d_{1}d_{2}\|\boldsymbol{\delta}_{x}\boldsymbol{\delta}_{y}\boldsymbol{\vartheta}_{x}\boldsymbol{\vartheta}_{y}\boldsymbol{c}^{0}\|_{xy}^{2},
\Phi^{k} := (1 + Q_{0}\tau)^{k} \Phi^{0} + \tau \sum_{l=1}^{k} (1 + Q_{0}\tau)^{k-l} \|\boldsymbol{f}^{l}\|^{2}, \quad k \geq 1,$$

and $Q_0 \ge 2$ is some positive constant to be specified.

First, for n = 1, (3.9) reduces to

$$\|\boldsymbol{\theta}_{x}\boldsymbol{\theta}_{y}\boldsymbol{c}^{1}\|^{2} + \frac{d_{1}d_{2}}{s_{1}\mu_{1}}\|\boldsymbol{\delta}_{x}\boldsymbol{\delta}_{y}\boldsymbol{\vartheta}_{x}\boldsymbol{\vartheta}_{y}\boldsymbol{c}^{1}\|_{xy}^{2}$$

$$\leq \frac{s_{1}}{\mu_{1}}\|\boldsymbol{\theta}_{x}\boldsymbol{\theta}_{y}\boldsymbol{c}^{0}\|^{2} + \frac{d_{1}d_{2}}{s_{1}\mu_{1}}\|\boldsymbol{\delta}_{x}\boldsymbol{\delta}_{y}\boldsymbol{\vartheta}_{x}\boldsymbol{\vartheta}_{y}\boldsymbol{c}^{0}\|_{xy}^{2} + \frac{1}{\mu_{1}}\|\boldsymbol{f}^{1}\|^{2}$$

$$\leq (1 + 2\tau)\Phi^{0} + \tau\|\boldsymbol{f}^{1}\|^{2},$$

which satisfies (3.11) for n = 1.

Second, we assume that (3.11) holds for all $n \le m-1$. By taking n=m in (3.9) we see

$$\tau \mu_{m} \|\boldsymbol{\theta}_{x} \boldsymbol{\theta}_{y} \boldsymbol{c}^{m}\|^{2} + \tau \frac{d_{1} d_{2}}{s_{m}} \|\boldsymbol{\delta}_{x} \boldsymbol{\delta}_{y} \boldsymbol{\vartheta}_{x} \boldsymbol{\vartheta}_{y} \boldsymbol{c}^{m}\|_{xy}^{2}$$

$$\leq \tau \sigma_{m} \|\boldsymbol{\theta}_{x} \boldsymbol{\theta}_{y} \boldsymbol{c}^{m-1}\|^{2} + \tau \frac{d_{1} d_{2}}{s_{m}} \|\boldsymbol{\delta}_{x} \boldsymbol{\delta}_{y} \boldsymbol{\vartheta}_{x} \boldsymbol{\vartheta}_{y} \boldsymbol{c}^{m-1}\|_{xy}^{2}$$

$$+ \frac{\lambda \tau}{\Gamma(1 + \alpha_{m})} \sum_{k=1}^{m-2} \left(b_{k+1}^{(m)} - b_{k}^{(m)}\right) \|\boldsymbol{\theta}_{x} \boldsymbol{\theta}_{y} \boldsymbol{c}^{k}\|^{2}$$

$$+ \frac{\lambda \tau b_{1}^{(m)}}{\Gamma(1 + \alpha_{m})} \|\boldsymbol{\theta}_{x} \boldsymbol{\theta}_{y} \boldsymbol{c}^{0}\|^{2} + \tau \|\boldsymbol{f}^{m}\|^{2}.$$
(3.12)

Note that

$$\frac{(2-2^{\alpha_{m-1}})\tau^{\alpha_{m-1}}}{\Gamma(1+\alpha_{m-1})} / \frac{(2-2^{\alpha_m})\tau^{\alpha_m}}{\Gamma(1+\alpha_m)} = \frac{2-2^{\alpha_{m-1}}}{2-2^{\alpha_m}} \cdot \frac{\Gamma(1+\alpha_m)}{\Gamma(1+\alpha_{m-1})} \cdot \tau^{\alpha_{m-1}-\alpha_m}, \quad (3.13)$$

and for enough small τ , we have

$$\frac{2^{\alpha_m}}{2^{\alpha_{m-1}}} = 2^{\alpha'(\xi_1)\tau} = \exp\left(\alpha'(\xi_1)\tau \ln 2\right) \le 1 + Q_1\tau$$

$$\Longrightarrow \frac{2 - 2^{\alpha_{m-1}}}{2 - 2^{\alpha_m}} \le \frac{2 - 2^{\alpha_{m-1}}}{2 - (1 + Q_1\tau)2^{\alpha_{m-1}}}$$

$$= 1 + \frac{Q_12^{\alpha_{m-1}}}{2 - (1 + Q_1\tau)2^{\alpha_{m-1}}}\tau \le 1 + Q_2\tau,$$

$$\frac{\Gamma(1+\alpha_m)}{\Gamma(1+\alpha_{m-1})} = 1 + \frac{\Gamma'(1+\alpha(\xi_2))\alpha'(\xi_2)}{\Gamma(1+\alpha_{m-1})}\tau \le 1 + Q_3\tau,
\tau^{\alpha_{m-1}-\alpha_m} = \tau^{-\alpha'(\xi_3)\tau} = \exp(-\alpha'(\xi_3)\tau \ln \tau)
= \exp(-\alpha'(\xi_3)\tau^{1-\alpha_*}\tau^{\alpha_*} \ln \tau) \le 1 + Q_4\tau^{1-\alpha_*},$$

where $\xi_i \in (t_{m-1}, t_m)$ and Q_i are positive constants for $1 \le i \le 4$. Thus, inserting these estimates into (3.13), we get

$$\frac{(2 - 2^{\alpha_{m-1}})\tau^{\alpha_{m-1}}}{\Gamma(1 + \alpha_{m-1})} \le \left(1 + 2Q_4\tau^{1-\alpha_*}\right) \frac{(2 - 2^{\alpha_m})\tau^{\alpha_m}}{\Gamma(1 + \alpha_m)},$$

and further we have

$$\frac{\sigma_{m-1}}{\sigma_{m}} \leq \left[\frac{1}{\tau} + \left(1 + 2Q_{4}\tau^{1-\alpha_{*}} \right) \frac{\lambda(2 - 2^{\alpha_{m}})\tau^{\alpha_{m}}}{\tau\Gamma(1 + \alpha_{m})} \right] \left[\frac{1}{\tau} + \frac{\lambda(2 - 2^{\alpha_{m}})\tau^{\alpha_{m}}}{\tau\Gamma(1 + \alpha_{m})} \right]^{-1} \\
\leq 1 + \left[2Q_{4}\tau^{1-\alpha_{*}} \frac{\lambda(2 - 2^{\alpha_{m}})\tau^{\alpha_{m}}}{\tau\Gamma(1 + \alpha_{m})} \right] \left[\frac{1}{\tau} + \frac{\lambda(2 - 2^{\alpha_{m}})\tau^{\alpha_{m}}}{\tau\Gamma(1 + \alpha_{m})} \right]^{-1} \\
\leq 1 + \left(2Q_{4} \frac{\lambda(2 - 2^{\alpha_{m}})}{\Gamma(1 + \alpha_{m})} \tau^{\alpha_{m} - \alpha_{*}} \right) \tau \leq 1 + Q_{5}\tau,$$

where in the last step we have used the fact that $\alpha_m \geq \alpha_*$, and the constant Q_5 is chosen such that

$$Q_5 \ge 2Q_4 \frac{\lambda(2 - 2^{\alpha_m})}{\Gamma(1 + \alpha_m)} \tau^{\alpha_m - \alpha_*}.$$

Moreover, we can prove that

$$\frac{s_{m-1}}{s_m} \le 1 + Q_5 \tau,$$

and thus, for τ sufficiently small, there exists a positive constant $Q_6 \geq 2Q_5$, such that

$$\frac{1}{s_m \sigma_m} \le (1 + Q_6 \tau) \frac{1}{s_{m-1} \sigma_{m-1}}.$$

With the above preliminary conclusions, we insert the induction hypothesis (3.11) into (3.12) to see

$$\tau \mu_{m} \|\boldsymbol{\theta}_{x} \boldsymbol{\theta}_{y} \boldsymbol{c}^{m}\|^{2} + \tau \frac{d_{1} d_{2}}{s_{m}} \|\boldsymbol{\delta}_{x} \boldsymbol{\delta}_{y} \boldsymbol{\vartheta}_{x} \boldsymbol{\vartheta}_{y} \boldsymbol{c}^{m}\|_{xy}^{2}$$

$$\leq \tau \sigma_{m} (1 + Q_{6} \tau) \left[\|\boldsymbol{\theta}_{x} \boldsymbol{\theta}_{y} \boldsymbol{c}^{m-1}\|^{2} + \frac{d_{1} d_{2}}{s_{m-1} \sigma_{m-1}} \|\boldsymbol{\delta}_{x} \boldsymbol{\delta}_{y} \boldsymbol{\vartheta}_{x} \boldsymbol{\vartheta}_{y} \boldsymbol{c}^{m-1}\|_{xy}^{2} \right]$$

$$+ \frac{\lambda \tau}{\Gamma (1 + \alpha_{m})} \sum_{k=1}^{m-2} \left(b_{k+1}^{(m)} - b_{k}^{(m)} \right) \|\boldsymbol{\theta}_{x} \boldsymbol{\theta}_{y} \boldsymbol{c}^{k}\|^{2} + \frac{\lambda \tau b_{1}^{(m)}}{\Gamma (1 + \alpha_{m})} \|\boldsymbol{\theta}_{x} \boldsymbol{\theta}_{y} \boldsymbol{c}^{0}\|^{2} + \tau \|\boldsymbol{f}^{m}\|^{2}$$

$$\leq \tau \sigma_{m} (1 + Q_{6} \tau) \Phi^{m-1} + \frac{\lambda \tau}{\Gamma (1 + \alpha_{m})} \sum_{k=1}^{m-2} \left(b_{k+1}^{(m)} - b_{k}^{(m)} \right) \Phi^{k}$$

$$+ \frac{\lambda \tau b_{1}^{(m)}}{\Gamma(1+\alpha_{m})} \|\boldsymbol{\theta}_{x} \boldsymbol{\theta}_{y} \boldsymbol{c}^{0}\|^{2} + \tau \|\boldsymbol{f}^{m}\|^{2}$$

$$\leq \left(\tau \sigma_{m} (1+Q_{6}\tau) + \frac{\lambda \tau}{\Gamma(1+\alpha_{m})} \sum_{k=1}^{m-2} \left(b_{k+1}^{(m)} - b_{k}^{(m)}\right) + \frac{\lambda \tau b_{1}^{(m)}}{\Gamma(1+\alpha_{m})}\right) \Phi^{m-1} + \tau \|\boldsymbol{f}^{m}\|^{2}$$

$$\leq \tau s_{m} (1+Q_{6}\tau) \Phi^{m-1} + \tau \|\boldsymbol{f}^{m}\|^{2}. \tag{3.14}$$

Then, divided by $\tau \mu_m$ on both sides of (3.14), together with the inequalities in (3.10) and choosing $Q_0 \ge 2(Q_6 + 2)$ such that

$$(1+2\tau)(1+Q_6\tau) \le 1 + Q_0\tau,$$

we get

$$\|\boldsymbol{\theta}_x\boldsymbol{\theta}_y\boldsymbol{c}^m\|^2 + \frac{d_1d_2}{s_m\mu_m}\|\boldsymbol{\delta}_x\boldsymbol{\delta}_y\boldsymbol{\vartheta}_x\boldsymbol{\vartheta}_y\boldsymbol{c}^m\|_{xy}^2 \le (1+Q_0\tau)\Phi^{m-1} + \tau\|\boldsymbol{f}^m\|^2 = \Phi^m,$$

which completes the induction (3.11) for n = m.

Finally, note that $(1 + Q_0\tau)^k$ in (3.11) is always bounded from up for sufficiently small τ , this together with (3.8) and Lemma 3.3 imply the conclusion.

3.2. Convergence of the ADI-QSC-*L*1 scheme

In this subsection, we consider the convergence of the proposed ADI-QSC-L1 scheme (2.19) for the approximation of (2.1).

Lemma 3.4 ([29]). Let $\Delta_c = \{X_{i,j}\}$ be the collocation points described in (2.9). Let $g_I(X) \in \mathcal{M}_x \otimes \mathcal{M}_y$ be the quadratic spline interpolation of function g(X), satisfying

$$g_I(X_{i,j}) = g(X_{i,j}), \quad (i,j) \in \bar{\omega}.$$
 (3.15)

Then, for $g(X) \in C^4(\bar{\Omega})$, the interpolation errors $g_I - g$ can be bounded by

$$\|\partial_x (g_I - g)\|_{\infty} = \mathcal{O}(h^2), \qquad \|\partial_y (g_I - g)\|_{\infty} = \mathcal{O}(h^2),$$
$$|\partial_{xx} (g_I - g)(\xi_i^x, \cdot)| = \mathcal{O}(h^2), \quad |\partial_{yy} (g_I - g)(\cdot, \xi_j^y)| = \mathcal{O}(h^2)$$

for
$$i = 0, 1, ..., N_x + 1$$
, $j = 0, 1, ..., N_y + 1$.

Theorem 3.2 (Convergence). Let $u^n = \{u_{i,j}^n\}$ and $U^n = \{U_{i,j}^n\}$, where $u_{i,j}^n$ is the exact solution of model (2.1) at $(X_{i,j},t_n)$, and $U_{i,j}^n = U^n(X_{i,j})$ in the form (2.8) is the solution of the ADI-QSC-L1 scheme (2.19). Then, we have

$$\|\boldsymbol{u}^n - \boldsymbol{U}^n\| \le Q\left(\tau + h^2\right),$$

where Q is a positive constant independent of h and τ .

Proof. Let $u_I^n(X) \in \mathcal{M}_x \otimes \mathcal{M}_y$ be the quadratic spline interpolation of $u^n(X)$ defined by (3.15). Then, it can be expressed as

$$u_I^n(X) = \sum_{i=0}^{N_x+1} \sum_{j=0}^{N_y+1} \bar{c}_{i,j}^n \phi_i(x) \phi_j(y).$$
 (3.16)

Besides, at collocation points, we have

$$(U^n - u^n)(X_{i,j}) = (U^n - u_I^n)(X_{i,j}), \quad (i,j) \in \bar{\omega}.$$
(3.17)

Similar as the construction process of the ADI-QSC-L1 method (2.19), it can be verified that the interpolation function $u_I^n(X)$ represented in (3.16) satisfies the following equation:

$$\begin{cases}
\delta_{\tau}\boldsymbol{\theta}_{x}\boldsymbol{\theta}_{y}\bar{c}_{i,j}^{n} + \lambda\delta_{\tau}^{1-\alpha_{n}}\boldsymbol{\theta}_{x}\boldsymbol{\theta}_{y}\bar{c}_{i,j}^{n} + \frac{d_{1}d_{2}}{s_{n}}\boldsymbol{\eta}_{x}\boldsymbol{\eta}_{y}\bar{c}_{i,j}^{n} \\
= d_{1}\boldsymbol{\eta}_{x}\boldsymbol{\theta}_{y}\bar{c}_{i,j}^{n} + d_{2}\boldsymbol{\theta}_{x}\boldsymbol{\eta}_{y}\bar{c}_{i,j}^{n} + \frac{d_{1}d_{2}}{s_{n}}\boldsymbol{\eta}_{x}\boldsymbol{\eta}_{y}\bar{c}_{i,j}^{n-1} + f_{i,j}^{n} + g_{i,j}^{n}, & (i,j) \in \omega, \\
\boldsymbol{\theta}_{x}\boldsymbol{\theta}_{y}\bar{c}_{i,j}^{n} = \varphi_{i,j}^{n}, & (i,j) \in \partial\omega, \\
\boldsymbol{\theta}_{x}\boldsymbol{\theta}_{y}\bar{c}_{i,j}^{0} = u_{i,j}^{o}, & (i,j) \in \bar{\omega},
\end{cases}$$
(3.18)

where

$$g_{i,j}^{n} := \delta_{\tau}(u_{I}^{n} - u^{n})(X_{i,j}) - r_{1,n} + \lambda \delta_{\tau}^{1-\alpha_{n}}(u_{I}^{n} - u^{n})(X_{i,j}) - \lambda r_{2,n}$$
$$- d_{1}\partial_{xx}(u_{I}^{n} - u^{n})(X_{i,j}) - d_{2}\partial_{yy}(u_{I}^{n} - u^{n})(X_{i,j})$$
$$+ \frac{d_{1}d_{2}}{s_{n}}\partial_{xxyy}(u_{I}^{n} - u_{I}^{n-1})(X_{i,j}),$$

and $r_{1,n}$ and $r_{2,n}$ are defined in (2.3)-(2.4), respectively. It is proved in [50] that $\partial_t u(X,\cdot) \in C[0,T]$, this together with $s_n = \mathcal{O}(\tau^{-1})$ and Lemma 3.4 show that

$$|g_{i,j}^n| = |r_{1,n}| + \lambda |r_{2,n}| + \mathcal{O}(\tau^2 + h^2), \quad (i,j) \in \omega.$$
 (3.19)

Let $e_{i,j}^n := \overline{c}_{i,j}^n - c_{i,j}^n$. Then, subtracting (2.19) from (3.18) we obtain the following error equation:

$$\begin{cases} \delta_{\tau}\boldsymbol{\theta}_{x}\boldsymbol{\theta}_{y}e_{i,j}^{n} + \lambda\delta_{\tau}^{1-\alpha_{n}}\boldsymbol{\theta}_{x}\boldsymbol{\theta}_{y}e_{i,j}^{n} + \frac{d_{1}d_{2}}{s_{n}}\boldsymbol{\eta}_{x}\boldsymbol{\eta}_{y}e_{i,j}^{n} \\ = d_{1}\boldsymbol{\eta}_{x}\boldsymbol{\theta}_{y}e_{i,j}^{n} + d_{2}\boldsymbol{\theta}_{x}\boldsymbol{\eta}_{y}e_{i,j}^{n} + \frac{d_{1}d_{2}}{s_{n}}\boldsymbol{\eta}_{x}\boldsymbol{\eta}_{y}e_{i,j}^{n} + g_{i,j}^{n}, & (i,j) \in \omega, \\ \boldsymbol{\theta}_{x}\boldsymbol{\theta}_{y}e_{i,j}^{n} = 0, & (i,j) \in \partial\omega, \\ \boldsymbol{\theta}_{x}\boldsymbol{\theta}_{y}e_{i,j}^{0} = 0, & (i,j) \in \bar{\omega}, \end{cases}$$

which can be rewritten as

$$\begin{cases} \left(\boldsymbol{\theta}_{x} - \frac{d_{1}}{s_{n}}\boldsymbol{\eta}_{x}\right) \left(\boldsymbol{\theta}_{y} - \frac{d_{2}}{s_{n}}\boldsymbol{\eta}_{y}\right) e_{i,j}^{n} = \frac{d_{1}d_{2}}{s_{n}^{2}}\boldsymbol{\eta}_{x}\boldsymbol{\eta}_{y}e_{i,j}^{n-1} + H_{i,j}^{n}, & (i,j) \in \omega, \\ \boldsymbol{\theta}_{x}\boldsymbol{\theta}_{y}e_{i,j}^{n} = 0, & (i,j) \in \partial\omega, \\ \boldsymbol{\theta}_{x}\boldsymbol{\theta}_{y}e_{i,j}^{0} = 0, & (i,j) \in \bar{\omega}, \end{cases}$$

$$(3.20)$$

where

$$H_{i,j}^{n} = \frac{1}{s_{n}\tau} \boldsymbol{\theta}_{x} \boldsymbol{\theta}_{y} e_{i,j}^{n-1} + \frac{\lambda}{s_{n}\Gamma(1+\alpha_{n})} \left[\sum_{k=1}^{n-1} (b_{k+1}^{(n)} - b_{k}^{(n)}) \boldsymbol{\theta}_{x} \boldsymbol{\theta}_{y} e_{i,j}^{k} + b_{1}^{(n)} \boldsymbol{\theta}_{x} \boldsymbol{\theta}_{y} e_{i,j}^{0} \right] + \frac{1}{s_{n}} g_{i,j}^{n}.$$

With a similar treatment as the proof of Theorem 3.1 for (3.20), we obtain

$$\|\boldsymbol{U}^{n} - \boldsymbol{u}_{I}^{n}\|^{2} = \|\boldsymbol{\theta}_{x}\boldsymbol{\theta}_{y}\boldsymbol{e}^{n}\|^{2}$$

$$\leq 2\tau \sum_{l=1}^{n} (1 + Q_{0}\tau)^{n-l}(\boldsymbol{g}^{l}, \boldsymbol{\theta}_{x}\boldsymbol{\theta}_{y}\boldsymbol{e}^{l})$$

$$\leq 2Q\tau \sum_{l=1}^{n} \|\boldsymbol{g}^{l}\| \|\boldsymbol{\theta}_{x}\boldsymbol{\theta}_{y}\boldsymbol{e}^{l}\|.$$
(3.21)

For simplicity, denote $E^n := \|\boldsymbol{\theta}_x \boldsymbol{\theta}_y \boldsymbol{e}^n\|$ for $n = 1, \dots, N_t$, and assume that there exist a $n_0 \in [1, N_t]$ such that $E^{n_0} := \max_{1 \le n \le N_t} E^n$. Then, we obtain from (3.21) that

$$\|\boldsymbol{U}^n - \boldsymbol{u}_I^n\|^2 = (E^n)^2 \le (E^{n_0})^2 = \|\boldsymbol{\theta}_x \boldsymbol{\theta}_y e^{n_0}\|^2 \le 2Q\tau E^{n_0} \sum_{l=1}^{n_0} \|\boldsymbol{g}^l\|,$$

which further implies that

$$\|\boldsymbol{U}^{n} - \boldsymbol{u}_{I}^{n}\| = E^{n} \le E^{n_0} \le 2Q\tau \sum_{l=1}^{n_0} \|\boldsymbol{g}^{l}\| \le 2Q\tau \sum_{l=1}^{N_t} \|\boldsymbol{g}^{l}\|.$$
 (3.22)

Then, by (3.19) and the estimates of $r_{1,n}$ and $r_{2,n}$ in (2.6)-(2.7), if $\alpha(0) = 1$, we have

$$\tau \sum_{l=1}^{N_t} \|\mathbf{g}^l\| \le Q\tau \sum_{l=1}^{N_t} (\tau + h^2) = \mathcal{O}(\tau + h^2).$$
 (3.23)

Otherwise,

$$\tau \sum_{l=1}^{N_t} \|\boldsymbol{g}^l\| \le Q\tau \sum_{l=1}^{N_t} \left(l^{-\alpha(0)} N_t^{\alpha(0)-1} + \lambda l^{-\alpha^*} N_t^{\alpha^*-1} + \tau^2 + h^2 \right)$$

$$\le Q\tau \int_0^1 \left(t^{-2\alpha(0)} + t^{-2\alpha^*} \right) dt + Q(\tau^2 + h^2) = \mathcal{O}(\tau + h^2). \tag{3.24}$$

Inserting (3.23)-(3.24) into (3.22) and using (3.17) finishes the proof.

4. Efficient implementation of the ADI-QSC-L1 method

We can see that the implementation of the ADI-QSC-L1 method (2.14)-(2.18) at the current time level t_n , requires all the approximations at previous time levels, and

thus a huge memory requirement of order $\mathcal{O}(N_xN_yN_t)$ and computational cost of order $\mathcal{O}(N_xN_yN_t^2)$ are still needed. In this section, we shall apply the ESA technique, originally proposed in [45] for variable-order Caputo fractional derivative, to the proposed ADI-QSC-L1 method, which leads to a fast version ADI method, say the ADI-QSC-FL1 method.

At the first time level t_1 , the ADI-QSC-FL1 scheme is exactly the same as the ADI-QSC-L1 scheme (2.14)-(2.18). For $2 \le n \le N_t$, we have the following lemma for the fast approximation of ${}_0^C \mathcal{D}_t^{1-\alpha_n} w(t_n)$.

Lemma 4.1 ([45]). For $2 \le n \le N_t$ and a given absolute tolerance error ϵ , there exist a constant κ , integers \underline{N} and \overline{N} such that

$$\kappa = \frac{2\pi}{\log 3 + \alpha^* \log(\cos 1)^{-1} + \log \epsilon^{-1}},$$

$$\underline{N} = \left\lceil \frac{\log \epsilon + \log \Gamma(1 - \alpha_n)}{\kappa \alpha_*} \right\rceil,$$

$$\overline{N} = \left\lfloor \frac{\log N_t + \log \log \epsilon^{-1} + \log \alpha_* + 2^{-1}}{\kappa} \right\rfloor,$$

and the variable-order Caputo fractional derivative ${}_0^C \mathcal{D}_t^{1-\alpha_n} w(t_n)$ can be fast evaluated as

$$\Delta_{\tau}^{1-\alpha_{n}}w(t_{n}) := \frac{T^{\alpha_{n}-1}}{\Gamma(\alpha_{n})} \sum_{\ell=N+1}^{\overline{N}} \omega_{n,\ell}W_{n,\ell}[w] + \frac{\tau^{\alpha_{n}-1}}{\Gamma(1+\alpha_{n})} (w(t_{n}) - w(t_{n-1}))$$
(4.1)

with

$$\left| \delta_{\tau}^{1-\alpha_n} w(t_n) - \Delta_{\tau}^{1-\alpha_n} w(t_n) \right| \le \epsilon, \tag{4.2}$$

where

$$\omega_{n,\ell} = \frac{\kappa e^{\ell \kappa \alpha_n}}{\Gamma(1 - \alpha_n)}, \quad \varrho_{\ell} = e^{\ell \kappa},$$

and $W_{n,\ell}[w]$ can be computed recursively via

$$W_{n,\ell}[w] = e^{-\frac{\varrho_{\ell}(t_n - t_{n-1})}{T}} W_{n-1,\ell}[w] + T \left(e^{-\frac{\varrho_{\ell}(t_n - t_{n-1})}{T}} - e^{-\frac{\varrho_{\ell}(t_n - t_{n-2})}{T}} \right)$$

$$\times \frac{w(t_{n-1}) - w(t_{n-2})}{\varrho_{\ell}(t_{n-1} - t_{n-2})}$$
(4.3)

for $n = 2, 3, ..., N_t$, with $W_{1,\ell}[w] = 0$.

Remark 4.1. In contrast to (2.4) for the approximations of $\{{}_{0}^{C}\mathcal{D}_{t}^{1-\alpha_{n}}w(t_{n})\}_{n=1}^{N_{t}}$ which require $\mathcal{O}(N_{t})$ memory and $\mathcal{O}(N_{t}^{2})$ computational cost, the total memory requirement and computational cost for (4.1) respectively reduce to order $\mathcal{O}(\log^{2}N_{t})$ and $\mathcal{O}(N_{t}\log^{2}N_{t})$. This is because that the number of exponentials in (4.1), say $\overline{N} - \underline{N}$, is only of order $\mathcal{O}(\log^{2}N_{t})$, see Ref. [45]. Thus, the coefficients $\{\omega_{n,\ell}\}_{\ell=N+1}^{\overline{N}}$ and

 $\{W_{n,\ell}[w]\}_{\ell=N+1}^{\overline{N}}$ contribute to the major storage, while (4.3) shows that at each time step one can update the quantity $W_{n,\ell}$ recursively in only $\mathcal{O}(1)$ computational work for each fixed i. Therefore, the computational cost for (4.1) is of order $\mathcal{O}(\log^2 N_t)$ for each time level, which amounts for a total computational cost of order $\mathcal{O}(N_t \log^2 N_t)$ for the approximations $\{\Delta_{\tau}^{1-\alpha_n}w(t_n)\}$ at all time levels.

Now, inserting the expression (4.1) with $w(t_n)$ and $W_{n,\ell}[w]$ replaced by vectors $c^n = \{c_{i,j}^n\}$ and $W_{n,\ell}[c]$ into the QSC-L1 scheme (2.10a), we obtain

$$\left[s_{n}\boldsymbol{\theta}_{x}\boldsymbol{\theta}_{y}-d_{1}\boldsymbol{\eta}_{x}\boldsymbol{\theta}_{y}-d_{2}\boldsymbol{\theta}_{x}\boldsymbol{\eta}_{y}\right]c_{i,j}^{n}$$

$$=s_{n}\boldsymbol{\theta}_{x}\boldsymbol{\theta}_{y}c_{i,j}^{n-1}-\frac{\lambda T^{\alpha_{n}-1}}{\Gamma(\alpha_{n})}\sum_{\ell=N+1}^{\overline{N}}\omega_{n,\ell}\boldsymbol{\theta}_{x}\boldsymbol{\theta}_{y}(\boldsymbol{W}_{n,\ell}[\boldsymbol{c}])_{i,j}+f_{i,j}^{n},$$
(4.4)

where the matrix $W_{n,\ell}[c]$ is recursively given by (4.3) with $W_{1,\ell}[c] = 0$.

Then, by respectively adding the terms $(d_1d_2/s_n)\eta_x\eta_yc_{i,j}^n$ and $(d_1d_2/s_n)\eta_x\eta_yc_{i,j}^{n-1}$ to left and right side of (4.4), and dividing the resulting equation by s_n , we obtain the fast version ADI-QSC-FL1 scheme

$$\left[\boldsymbol{\theta}_{x}\boldsymbol{\theta}_{y} - \frac{d_{1}}{s_{n}}\boldsymbol{\eta}_{x}\boldsymbol{\theta}_{y} - \frac{d_{2}}{s_{n}}\boldsymbol{\theta}_{x}\boldsymbol{\eta}_{y} + \frac{d_{1}d_{2}}{s_{n}^{2}}\boldsymbol{\eta}_{x}\boldsymbol{\eta}_{y}\right]c_{i,j}^{n}$$

$$= \frac{d_{1}d_{2}}{s_{n}^{2}}\boldsymbol{\eta}_{x}\boldsymbol{\eta}_{y}c_{i,j}^{n-1} + \boldsymbol{\theta}_{x}\boldsymbol{\theta}_{y}c_{i,j}^{n-1} - \frac{\lambda T^{\alpha_{n}-1}}{s_{n}\Gamma(\alpha_{n})}\sum_{\ell=N+1}^{\overline{N}}\omega_{n,\ell}\boldsymbol{\theta}_{x}\boldsymbol{\theta}_{y}(\boldsymbol{W}_{n,\ell}[\boldsymbol{c}])_{i,j} + \frac{1}{s_{n}}f_{i,j}^{n} \quad (4.5)^{n}$$

for $2 \le n \le N_t$. In practical implementation, the ADI-QSC-FL1 scheme (4.5) reads as follows:

Step 1. For each $j = 1, 2, ..., N_y$, solve the following linear systems along x-direction:

$$\begin{cases}
\theta_{x}c_{0,j}^{*} = \left(\theta_{y} - \frac{d_{2}}{s_{n}}\eta_{y}\right)\theta_{x}c_{0,j}^{n}, \\
\left(\theta_{x} - \frac{1}{s_{n}}d_{1}\eta_{x}\right)c_{i,j}^{*} = \frac{d_{1}d_{2}}{s_{n}^{2}}\eta_{x}\eta_{y}c_{i,j}^{n-1} + \theta_{x}\theta_{y}c_{i,j}^{n-1} \\
-\frac{1}{s_{n}}\frac{\lambda_{n}T^{\alpha_{n}-1}}{\Gamma(\alpha_{n})}\sum_{\ell=\underline{N}+1}^{\overline{N}}\omega_{n,\ell}\theta_{x}\theta_{y}(W_{n,\ell}[c])_{i,j} + \frac{1}{s_{n}}f_{i,j}^{n}, \quad i = 1, 2, \dots, N_{x}, \\
\theta_{x}c_{N_{x}+1,j}^{*} = \left(\theta_{y} - \frac{d_{2}}{s_{n}}\eta_{y}\right)\theta_{x}c_{N_{x}+1,j}^{n},
\end{cases}$$

$$(4.6)$$

where $\{\theta_x c_{0,j}^n\}$ and $\{\theta_x c_{N_x+1,j}^n\}$ for $j=0,1,\ldots,N_y+1$ are obtained similarly as what we did in (2.15).

Step 2. For each $i = 1, 2, ..., N_x$, solve the following linear systems along y-direction:

$$\left(\boldsymbol{\theta}_{y} - \frac{d_{2}}{s_{n}}\boldsymbol{\eta}_{y}\right)c_{i,j}^{n} = c_{i,j}^{*}, \quad j = 1, 2, \dots, N_{y}$$

$$(4.7)$$

with boundary equations $\{\theta_y c_{i,0}^n\}$ and $\{\theta_y c_{i,N_y+1}^n\}$ determined similarly as (2.17). Moreover, $\{c_{0,j}^n\}$ and $\{c_{N_x+1,j}^n\}$ are also given by (2.18).

Remark 4.2. As seen in the ADI-QSC-FL1 scheme (4.5), the evaluation of the variable-order Caputo fractional derivative at the current time level only depends on the approximations at the current time interval $[t_{n-1},t_n]$ and its previous historical information that stored via the matrix $W_{n,\ell}[c]$ for each ℓ . Thus, the major memory requirement for the ADI-QSC-FL1 scheme (4.6)-(4.7) is the storage of such matrices for all $\ell=\underline{N}+1$ to \overline{N} . Therefore, the total memory requirement for the ADI-QSC-FL1 scheme is reduced to $\mathcal{O}(N_xN_y\log^2N_t)$ compared with the ADI-QSC-L1 scheme. Besides, note that at each time level, the ESA technique is only applied in the first step, which accounts for the computational cost of order $\mathcal{O}(N_xN_y\log^2N_t)$ as discussed in Remark 4.1, and meanwhile, only some linear tri-diagonal systems are solved in both steps, which can be solved by the Thomas algorithm in only $\mathcal{O}(N_xN_y)$ computational complexity. Therefore, the total computational cost for the ADI-QSC-L1 scheme is reduced to $\mathcal{O}(N_xN_yN_t\log^2N_t)$. It is clear that both the memory requirement and computational cost are much less than those for the ADI-QSC-L1 scheme developed in Section 2, especially for long time or small time stepsize modeling.

5. Numerical experiments

In this section, three different examples in two and three space dimensions are tested to verify the convergence orders of the ADI-QSC-L1 method and to show the efficiency of the fast version ADI-QSC-FL1 method. All programs are run on a Lenovo desktop with Intel(R) Core(TM) i7-7700 CPU @ 3.60GHz with Matlab R2017b.

Example 5.1. For the first example, we consider the two-dimensional model (2.1) on the space-time domain $[0,1]^2 \times [0,1]$, where the coefficients $\lambda = d_1 = d_2 = 1$ and the source function f(X,t) is chosen such that the true solution is $u(X,t) = (1+t^2)\cos(x)\cos(y)$.

In order to investigate the convergence orders of the developed methods, we consider the following three different types of variable-order $\alpha(t)$, i.e.:

$$\alpha_1(t) = \cos(0.4\pi t),$$

$$\alpha_2(t) = 0.5(1 + \sin(1.3\pi t)),$$

$$\alpha_3(t) = 0.4 + 0.6 \left[1 - t - \frac{\sin 2\pi (1 - t)}{2\pi}\right].$$

We first fix $N_x=N_y=256$ to observe the temporal convergence orders of ADI-QSC-L1 method. By doubling the values of N_t repeatedly from 32 to 256, we show the corresponding errors and convergence orders for different $\alpha(t)$ in Table 1. Next, by choosing $N_t=131072$ large enough, we test the spatial convergence orders in Table 2. We can see that the convergence orders displayed in Tables 1-2 fit the theoretical

Table 1: Errors and temporal convergence orders of the ADI-QSC-L1 method for Example 5.1.

	$\alpha_1(t)$			$\alpha_2(t)$			$\alpha_3(t)$		
N_t	Error	Order	N_t	Error	Order	N_t	Error	Order	
32	1.03e-03	_	32	1.28e-03	_	32	1.00e-03	_	
64	5.09e-04	1.02	64	6.26e-04	1.03	64	4.97e-04	1.01	
128	2.51e-04	1.02	128	3.06e-04	1.03	128	2.46e-04	1.02	
256	1.24e-04	1.02	256	1.50e-04	1.03	256	1.21e-04	1.02	
		≈ 1.00			≈ 1.00			≈ 1.00	

Table 2: Errors and spatial convergence orders of the ADI-QSC-L1 method for Example 5.1.

	$\alpha_1(t)$	$\alpha_2($	t)	$\alpha_3(t)$		
N	Error	Order	Error	Order	Error	Order
8	6.99e-05		7.00e-05		6.99e-05	_
16	1.76e-05	1.99	1.76e-05	1.99	1.76e-05	1.99
32	4.25e-06	2.05	4.23e-06	2.06	4.25e-06	2.05
64	8.93e-07	2.25	8.67e-07	2.29	8.94e-07	2.25
		≈ 2.00		≈ 2.00		≈ 2.00

Table 3: Comparisons of results obtained by different methods for Example 5.1.

		QSC-L1		ADI-QSC- $L1$		ADI-QSC-F L 1		1
N	N_t	Error	Time	Error	Time	N_{exp}	Error	Time
32	256	1.18e-04	1.17 s	1.17e-04	0.27 s	41	1.20e-04	0.36 s
64	512	5.92e-05	10 s	5.90e-05	1.58 s	51	6.14e-05	1.03 s
128	1024	2.96e-05	90 s	2.95e-05	18 s	63	3.17e-05	8 s
256	2048	1.47e-05	781 s	1.47e-05	195 s	75	1.71e-05	58 s
512	4096	7.35e-06	13589 s	7.34e-06	7406 s	89	9.58e-06	960 s

second-order spatial accuracy and first-order temporal accuracy very well. Finally, in order to show the strong performance of the ADI-QSC-FL1 method using the ESA technique, we run the direct QSC-L1 method (2.10), the ADI-QSC-L1 method (2.14)-(2.18) and the ADI-QSC-FL1 method (4.6)-(4.7) for comparisons. Numerical results including errors and CPU times for $\alpha_3(t)$ are displayed in Table 3, where $N_{exp} = \overline{N} - \underline{N}$ for the ESA technique. We can see that all methods generate the similar error results, while the ADI approach consumes much less CPU running time. Moreover, the ADI-QSC-FL1 method, which combines the ADI and ESA techniques, is able to further improve the computational efficiency greatly. For example, with $N_x = N_y = N = 512$ and $N_t = 4096$, all three methods yield numerical errors about magnitude 10^{-6} , but the running times have been reduced from 13589 seconds (= 3 hours 46 minutes 29 seconds) to 7406 seconds (2 hours 3 minutes 26 seconds) to 960 seconds (16 minutes) for the direct QSC-L1 method, the ADI-QSC-L1 method and the ADI-QSC-L1 method. Thus, the developed fast version ADI method shows strong potential in large-scale and long time modeling and simulations.

Example 5.2. In the second example, we consider a three-dimensional model (2.1) on the space-time domain $[0,1]^3 \times [0,1]$, where the coefficients $\lambda = d_1 = d_2 = d_3 = 1$ and f(X,t) is chosen such that the true smooth solution is

$$u(X,t) = (1+t^2)\cos(x)\cos(y)\cos(z).$$

The same variable-order functions $\alpha(t)$ as those in Example 5.1 are employed.

In this situation, the QSC schemes for the computation of $\{c_{i,j,k}^n\}$ at time level t_n can be developed similarly, but are more complicated. For example, the ADI-QSC-L1 scheme reads in the following three sub-steps:

Step 1. For each $j=1,2,\ldots,N_y$, $k=1,2,\ldots,N_z$, solve a series of (N_x+2) -by- (N_x+2) linear algebra systems along x-direction

$$\begin{cases}
\theta_{x}c_{0,j,k}^{*} = \left(\theta_{y} - \frac{d_{2}}{s_{n}}\eta_{y}\right)\left(\theta_{z} - \frac{d_{3}}{s_{n}}\eta_{z}\right)\theta_{x}c_{0,j,k}^{n}, \\
\left(\theta_{x} - \frac{d_{1}}{s_{n}}\eta_{x}\right)c_{i,j,k}^{*} = \tilde{F}_{i,j,k}^{n}, \quad i = 1, 2, \dots, N_{x}, \\
\theta_{x}c_{N_{x}+1,j,k}^{*} = \left(\theta_{y} - \frac{d_{2}}{s_{n}}\eta_{y}\right)\left(\theta_{z} - \frac{d_{3}}{s_{n}}\eta_{z}\right)\theta_{x}c_{N_{x}+1,j,k}^{n},
\end{cases} (5.1)$$

where $\{\theta_x c_{0,j,k}^n\}$ and $\{\theta_x c_{N_x+1,j,k}^n\}$ are respectively solved at boundaries $x=x_L$ and $x=x_R$ by

$$\theta_y \theta_z(\theta_x c_{0,j,k}^n) = \varphi(\xi_0^x, \xi_j^y, \xi_k^z, t_n),
\theta_y \theta_z(\theta_x c_{N_x+1,j,k}^n) = \varphi(\xi_{N_x+1}^x, \xi_j^y, \xi_k^z, t_n)$$
(5.2)

for $j = 0, 1, \dots, N_y + 1$ and $k = 0, 1, \dots, N_z + 1$.

Step 2. For each $i=1,2,\ldots,N_x$, $k=1,2,\ldots,N_z$, solve a series of (N_y+2) -by- (N_y+2) linear algebra systems along y-direction

$$\begin{cases}
\boldsymbol{\theta}_{y}c_{i,0,k}^{**} = \left(\boldsymbol{\theta}_{z} - \frac{d_{3}}{s_{n}}\boldsymbol{\eta}_{z}\right)\boldsymbol{\theta}_{y}c_{i,0,k}^{n}, \\
\left(\boldsymbol{\theta}_{y} - \frac{d_{2}}{s_{n}}\boldsymbol{\eta}_{y}\right)c_{i,j,k}^{**} = c_{i,j,k}^{*}, \quad j = 1, 2, \dots, N_{y}, \\
\boldsymbol{\theta}_{y}c_{i,N_{y}+1,k}^{**} = \left(\boldsymbol{\theta}_{z} - \frac{d_{3}}{s_{n}}\boldsymbol{\eta}_{z}\right)\boldsymbol{\theta}_{y}c_{i,N_{y}+1,k}^{n},
\end{cases} (5.3)$$

where $\{\theta_y c_{i,0,k}^n\}$ and $\{\theta_y c_{i,N_y+1,k}^n\}$ are respectively solved at boundaries $y=y_L$ and $y=y_R$ by

$$\theta_x \theta_z(\theta_y c_{i,0,k}^n) = \varphi(\xi_i^x, \xi_0^y, \xi_k^z, t_n),
\theta_x \theta_z(\theta_y c_{i,N_y+1,k}^n) = \varphi(\xi_i^x, \xi_{N_y+1}^y, \xi_k^z, t_n)$$
(5.4)

for $i = 0, 1, ..., N_x + 1$ and $k = 0, 1, ..., N_z + 1$.

Step 3. For each $i=1,2,\ldots,N_x, j=1,2,\ldots,N_y$, solve a series of (N_z+2) -by- (N_z+2) linear algebra systems along z-direction

$$\left(\boldsymbol{\theta}_{z} - \frac{d_{3}}{s_{n}} \boldsymbol{\eta}_{z}\right) c_{i,j,k}^{n} = c_{i,j,k}^{**}, \quad k = 1, 2, \dots, N_{z}$$
(5.5)

with boundary equations $\theta_z c_{i,j,0}^n$ and $\theta_z c_{i,j,N_z+1}^n$ determined at boundaries $z=z_L$ and $z=z_R$ by

$$\theta_x \theta_y(\theta_z c_{i,j,0}^n) = \varphi(\xi_i^x, \xi_j^y, \xi_0^z, t_n),
\theta_x \theta_y(\theta_z c_{i,i,N_z+1}^n) = \varphi(\xi_i^x, \xi_j^y, \xi_{N_z+1}^z, t_n)$$
(5.6)

for $i = 0, 1, \dots, N_x + 1$ and $j = 0, 1, \dots, N_u + 1$.

Finally, using the data $\{\theta_x c^n_{0,j,k}\}$ and $\{\theta_x c^n_{N_x+1,j,k}\}$ determined by (5.2), the quantities $\{c^n_{0,j,k}\}$ and $\{c^n_{N_x+1,j,k}\}$ corresponding to the boundaries $x=x_L$ and $x=x_R$ are given by

$$c_{0,j,k}^{n} = 2\boldsymbol{\theta}_{x}c_{0,j,k}^{n} - c_{1,j,k}^{n}, \quad c_{N_{x}+1,j,k}^{n} = 2\boldsymbol{\theta}_{x}c_{N_{x}+1,j,k}^{n} - c_{N_{x},j,k}^{n}$$
(5.7)

for $j=1,\ldots,N_y$ and $k=1,\ldots,N_z$. Likewise, the quantities $\{c_{i,0,k}^n\}$ and $\{c_{i,N_y+1,k}^n\}$ corresponding to the boundaries $y=y_L$ and $y=y_R$ are given by

$$c_{i,0,k}^n = 2\boldsymbol{\theta}_y c_{i,0,k}^n - c_{i,1,k}^n, \quad c_{i,N_y+1,k}^n = 2\boldsymbol{\theta}_y c_{i,N_y+1,k}^n - c_{i,N_y,k}^n$$
(5.8)

for $i = 1, ..., N_x$ and $k = 1, ..., N_z$.

At the four edges $(\xi_i^x, \xi_j^y, \xi_k^z)$ for $i = \{0, N_x + 1\}$ and $j = \{0, N_y + 1\}$, we have

$$\theta_z(\theta_x \theta_y c_{i,i,k}^n) = \varphi(\xi_i^x, \xi_i^y, \xi_k^z, t_n), \quad k = 0, 1, \dots, N_z + 1.$$

$$(5.9)$$

By solving the above four linear systems of order (N_z+2) -by- (N_z+2) , we then obtain the quantities at four corners

$$c_{0,0,k}^{n} = 4\theta_{x}\theta_{y}c_{0,0,k}^{n} - c_{0,1,k}^{n} - c_{1,0,k}^{n} - c_{1,1,k}^{n},$$

$$c_{0,N_{y}+1,k}^{n} = 4\theta_{x}\theta_{y}c_{0,N_{y}+1,k}^{n} - c_{1,N_{y}+1,k}^{n} - c_{0,N_{y},k}^{n} - c_{1,N_{y},k}^{n},$$

$$c_{N_{x}+1,0,k}^{n} = 4\theta_{x}\theta_{y}c_{N_{x}+1,0,k}^{n} - c_{N_{x},0,k}^{n} - c_{N_{x}+1,1,k}^{n} - c_{N_{x},1,k}^{n},$$

$$c_{N_{x}+1,N_{y}+1,k}^{n} = 4\theta_{x}\theta_{y}c_{N_{x}+1,N_{y}+1,k}^{n} - c_{N_{x},N_{y}+1,k}^{n} - c_{N_{x}+1,N_{y},k}^{n} - c_{N_{x},N_{y},k}^{n}$$

$$(5.10)$$

for $k = 0, 1, \dots, N_z + 1$.

In the following run of (5.1)-(5.10), we first fix $N_x = N_y = N_z = N = 64$ and show the corresponding errors and convergence orders for different $\alpha(t)$ in Table 4. Then, we choose $N_t = 131072$, and test the spatial convergence orders in Table 5. We can also see that the convergence orders displayed in Tables 4-5 fit the theoretical second-order spatial accuracy and first-order temporal accuracy pretty well. Besides, we also compare the performance of the ADI-QSC-FL1 method with the ADI-QSC-L1 method and the direct QSC-L1 method. Numerical results are presented in Table 6. It can be seen that, the ADI strategy and the ESA acceleration technique are able to improve the efficiency of the QSC-L1 method greatly.

Table 4: Errors and temporal convergence orders of the ADI-QSC-L1 method for Example 5.2.

	$\alpha_1(t)$		$\alpha_2(t)$			$\alpha_3(t)$		
N_t	Error	Order	N_t	Error	Order	N_t	Error	Order
32	5.03e-04	_	32	6.56e-04	-	32	4.83e-04	-
64	2.58e-04	0.96	64	3.31e-04	0.99	64	2.49e-04	0.96
128	1.29e-04	1.00	128	1.64e-04	1.01	128	1.25e-04	0.99
256	6.39e-05	1.01	256	8.02e-05	1.03	256	6.22e-05	1.01
		≈ 1.00			≈ 1.00			≈ 1.00

Table 5: Errors and spatial convergence orders of the ADI-QSC-L1 method for Example 5.2.

	$\alpha_1(t)$	α_2	t)	$\alpha_3(t)$		
N	Error	Order	Error	Order	Error	Order
4	2.14e-04		2.14e-04	_	2.14e-04	_
8	5.63e-05	1.93	5.63e-05	1.93	5.63e-05	1.93
16	1.39e-05	2.02	1.38e-05	2.03	1.39e-05	2.02
32	3.13e-06	2.15	3.05e-06	2.18	3.13e-06	2.15
		≈ 2.00		≈ 2.00		≈ 2.00

Table 6: Comparisons of results obtained by different methods for Example 5.2 with $\alpha_3(t)$.

		QSC-L1		ADI-QSC- $L1$		ADI-QSC-F $L1$		
N	N_t	Error	Time	Error	Time	N_{exp}	Error	Time
16	512	1.74e-05	53 s	1.71e-05	7 s	18	1.75e-05	6 s
32	1024	1.21e-05	2775 s	1.20e-05	89 s	22	1.14e-05	65 s
48	2048	6.18e-06	42859 s	6.16e-06	604 s	26	5.90e-06	330 s
64	4096	_	_	2.96e-06	9050 s	31	3.31e-06	1567 s

Example 5.3. In the last example, we apply the developed fast version ADI method for the dynamic evolution modeling of variable-order time-fractional Allen-Cahn equation [19]

$${}_{0}^{C}\mathcal{D}_{t}^{\alpha(t)}\phi - \varepsilon^{2}\Delta\phi + \phi(\phi^{2} - 1) = 0 \quad \text{in } \Omega \times (0, T] := (-1, 1)^{2} \times (0, 200]$$
 (5.11)

with the interface width $\varepsilon = 0.02$. The initial condition of (5.11) is chosen as

$$\phi(x,y,0) = -0.9 \tanh\left(\frac{(x-0.3)^2 + y^2 - 0.04}{\varepsilon}\right) \tanh\left(\frac{(x+0.3)^2 + y^2 - 0.04}{\varepsilon}\right)$$

$$\times \tanh\left(\frac{x^2 + (y-0.3)^2 - 0.04}{\varepsilon}\right) \tanh\left(\frac{x^2 + (y+0.3)^2 - 0.04}{\varepsilon}\right),$$

and the fractional order is taken as

$$\alpha(t) = 0.5 + 0.4 \left[1 - \frac{t}{200} - \frac{\sin(2\pi(1 - t/200))}{2\pi} \right].$$

We use this model to simulate the merging of four-drops on the interface. In the implementation of the ADI-QSC-L1 method, the nonlinear term is handled explicitly, and a stabilized term is added from the second time instant, i.e.

$$\begin{cases}
\left(\boldsymbol{\theta}_{x} - \frac{\varepsilon^{2}}{r_{n}}\boldsymbol{\eta}_{x}\right)c_{i,j}^{n,*} = \frac{\varepsilon^{4}}{r_{n}^{2}}\boldsymbol{\eta}_{x}\boldsymbol{\eta}_{y}c_{i,j}^{n-1} + G_{i,j}^{n} - \frac{S}{r_{n}}\boldsymbol{\theta}_{x}\left(c_{i,j}^{n,*} - c_{i,j}^{n-1,*}\right), & n \geq 2, \\
\left(\boldsymbol{\theta}_{y} - \frac{\varepsilon^{2}}{r_{n}}\boldsymbol{\eta}_{y}\right)c_{i,j}^{n} = c_{i,j}^{n,*},
\end{cases}$$

where S is a user-defined stabilized constant, and

$$G_{i,j}^n := \frac{1}{b_n^{(n)}} \left[\sum_{k=1}^{n-1} \left(b_{k+1}^{(n)} - b_k^{(n)} \right) \phi_{i,j}^k + b_1^{(n)} \phi_{i,j}^0 \right] - \frac{1}{r_n} \phi_{i,j}^{n-1} \left[\left(\phi_{i,j}^{n-1} \right)^2 - 1 \right], \quad r_n = \frac{b_n^{(n)}}{\Gamma(1+\alpha_n)}.$$

In order to reduce the computational cost, we choose the following adaptive temporal stepsize strategy:

$$\tau_{n+1} = \max \left\{ \tau_{\min}, \frac{\tau_{\max}}{\sqrt{1 + \eta \|\delta_{\tau} \phi^n\|^2}} \right\}$$

with $\tau_{\rm min}=4.0\times10^{-3}$, $\tau_{\rm max}=1$ and $\eta=1.9\times10^4$ [33]. The profiles of the phase function ϕ obtained by direct QSC-L1 method and time adaptive ADI-QSC-L1 method at time instants t=1,50,100,200 are shown in Fig. 1 for $N_x=N_y=256$, and the number of time steps and the CPU running time are shown in Table 7. It can be seen that the four-drops gradually merge, and the time adaptive ADI-QSC-L1 method behaves almost the same as the direct QSC-L1 method with $\tau=\tau_{\rm min}$, while consume only the almost same running time as that with $\tau=\tau_{\rm max}$.

Moreover, we also investigate the evolution of the Ginzburg-Landau free energy

$$E[u](t) = \int_{\Omega} \left(\frac{\varepsilon^2}{2} |\nabla \phi|^2 + \frac{1}{4} (1 - \phi^2)^2 \right) dx dy.$$

In order to observe the relationship between the energy functional and the fractional orders, we also introduce several different fractional orders

$$\alpha_2(t) \equiv 0.5,$$

$$\alpha_3(t) = 0.4 \left[1 + \sin\left(\frac{1.3\pi t}{200}\right) \right],$$

$$\alpha_4(t) = 0.6 - 0.4 \left[1 - \frac{t}{200} - \frac{\sin(2\pi(1 - t/200))}{2\pi} \right],$$

Table 7: The number of time steps and CPU time obtained by different methods for Example 5.3.

	QSC- $L1$ with $\tau=1$	QSC- $L1$ with $\tau = 4.0e-3$	Adaptive ADI-QSC-L1
# of steps	200	50000	1080
CPU time	17 s	36815 s	20 s

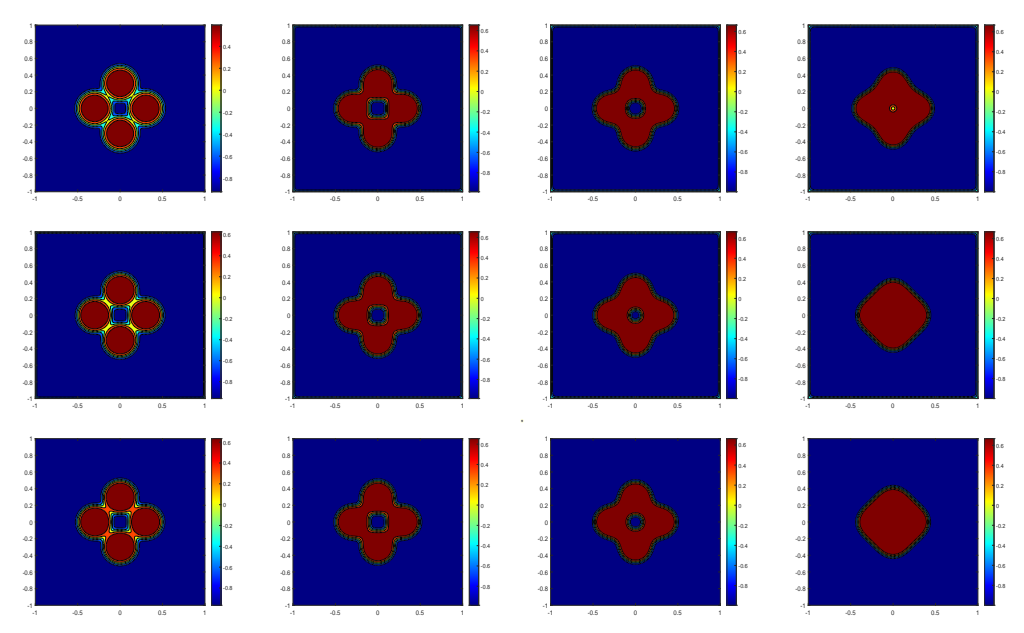


Figure 1: Solution snapshots of Example 5.3 at t=1,50,100,200 (from left to right), for direct method with $\tau=\tau_{\rm max}$ (top) and $\tau=\tau_{\rm min}$ (middle), and time adaptive ADI-QSC-L1 method (bottom).

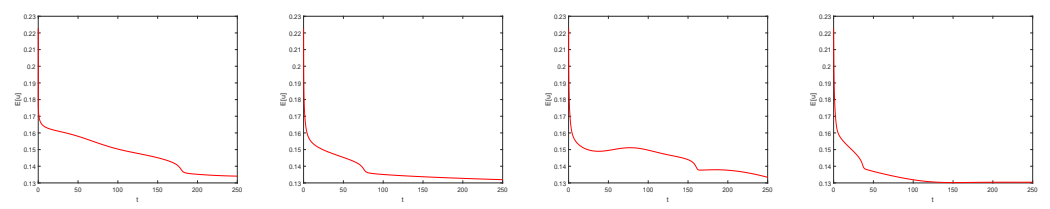


Figure 2: Discrete energy functional generated by the time adaptive ADI-QSC-FL1 method for Example 5.3 with fractional orders $\alpha(t)$, $\alpha_2(t)$, $\alpha_3(t)$, $\alpha_4(t)$ (from left to right).

where $\alpha_2(t)$ is a constant order, and $\alpha_4(t)$ is a monotonically increasing function. The discrete energy functionals obtained by the time adaptive ADI-QSC-FL1 method for different fractional orders are shown in Fig. 2. We can see that generally it decays if the variable fractional orders are constant or monotonic functions, such as $\alpha(t)$, $\alpha_2(t)$ and $\alpha_4(t)$. However, for the case $\alpha_3(t)$, though the discrete energy functional tends to be stable, it is not always decreasing. There is still a big mathematical theory gap whether the variable-order time-fractional Allen-Cahn equation is energy-dissipating or not.

6. Concluding remarks

In this paper, we first develop a QSC-L1 method for the two-dimensional variable-order time-fractional mobile-immobile diffusion equation, and then by adding small perturbation terms, an ADI-QSC-L1 method is further proposed. With some prepared fundamental lemmas, we prove that the method is unconditionally stable and conver-

gent with order $\mathcal{O}(\tau+h^2)$ in discrete L_2 norm, see Theorems 3.1-3.2. Then, combined with the ESA technique, a fast version of the ADI-QSC-L1 method, named ADI-QSC-L1, is proposed to further improve the computational efficiency. The proposed method is also applicable to model (2.1) in three space dimensions. Numerical examples are provided to verify the theoretical findings. We show that the ADI strategy is able to reduce the running time greatly, while preserves almost the same level of observing errors, and the ESA acceleration technique can further improve the computational efficiency. Meanwhile, numerical experiments also show that the developed ADI-QSC methods are applicable to model phase field equations. However, it is still not sure whether there is an energy-dissipating law for the variable-order time-fractional Allen-Cahn equation.

Acknowledgements

This work was supported in part by the National Key R&D Program of China (Grant No. 2023YFA1009003), by the National Natural Science Foundation of China (Grant Nos. 11971482, 12131014), by the Shandong Provincial Natural Science Foundation (Grant Nos. ZR2024MA023, ZR2021MA020, ZR2020MA039, ZR2023MA081), and by the Fundamental Research Funds for the Central Universities (Grant Nos. 22CX03016A, 202264006).

References

- [1] A. A. ALIKHANOV, A new difference scheme for the time fractional diffusion equation, J. Comput. Phys. 280 (2015), 424–438.
- [2] Y. Chen, X. Lin, M. Zhang, and Y. Huang, Stability and convergence of L1-Galerkin spectral methods for the nonlinear time fractional cable equation, East Asian J. Appl. Math. 13 (2023), 22–46.
- [3] Y. CHEN, X. TAN, AND Y. HUANG, $L2-1\sigma$ finite element method for time-fractional diffusion problems with discontinuous coefficients, East Asian J. Appl. Math. 13 (2023), 813–834.
- [4] C. C. Christara, Quadratic spline collocation methods for elliptic partial differential equations, BIT 34 (1994), 33–61.
- [5] C. C. Christara, T. Chen, and D. M. Dang, Quadratic spline collocation for one-dimensional parabolic partial differential equations, Numer. Algor. 53 (2010), 511–553.
- [6] G. FAIRWEATHER, X. YANG, D. Xu, AND H. ZHANG, An ADI Crank-Nicolson orthogonal spline collocation method for the two-dimensional fractional diffusion-wave equation, J. Sci. Comput. 65 (2015), 1217–1239.
- [7] H. Fu, H. Liu, AND H. Wang, A finite volume method for two-dimensional Riemann-Liouville space-fractional diffusion equation and its efficient implementation, J. Comput. Phys. 388 (2019), 316–334.
- [8] H. Fu, Y. Sun, H. Wang, and X. Zheng, Stability and convergence of a Crank-Nicolson finite volume method for space fractional diffusion equations, Appl. Numer. Math. 139 (2019), 38–51.

[9] D. Hou, Z. Qiao, and T. Tang, Fast high order and energy dissipative schemes with variable time steps for time-fractional molecular beam epitaxial growth model, Ann. Appl. Math. 39 (2023), 429–4610.

- [10] E. N. HOUSTIS, C. C. CHRISTARA, AND J. R. RICE, Quadratic-spline collocation methods for two-point boundary value problems, Int. J. Numer. Meth. Eng. 26 (1988), 935–952.
- [11] C. JI AND W. DAI, Numerical algorithm with fourth-order spatial accuracy for solving the time-fractional dual-phase-lagging nanoscale heat conduction equation, Numer. Math. Theor. Meth. Appl. 16 (2023), 511–540.
- [12] S. JIANG, J. ZHANG, Q. ZHANG, AND Z. ZHANG, Fast evaluation of the Caputo fractional derivative and its applications to fractional diffusion equations, Commun. Comput. Phys. 21 (2017), 650–678.
- [13] B. JIN, R. LAZAROV, J. PASCIAK, AND Z. ZHOU, Error analysis of a finite element method for the space-fractional parabolic equation, SIAM J. Numer. Anal. 52 (2014), 2272–2294.
- [14] C. LI AND H. DING, *Higher order finite difference method for the reaction and anomalous-diffusion equation*, Appl. Math. Model. 38 (2014), 3802–3821.
- [15] C. LI AND Z. WANG, *L1/Local discontinuous Galerkin method for the time-fractional Stokes equation*, Numer. Math. Theor. Meth. Appl. 15 (2022), 1099–1127.
- [16] C. LI, T. ZHAO, W. DENG, AND Y. WU, Orthogonal spline collocation methods for the subdiffusion equation, J. Comput. Appl. Math. 255 (2014), 517–528.
- [17] Z. LI, H. WANG, R. XIAO, AND S. YANG, A variable-order fractional differential equation model of shape memory polymers, Chaos Soliton. Fract. 102 (2017), 473–485.
- [18] H. LIANG AND M. STYNES, A general collocation analysis for weakly singular Volterra integral equations with variable exponent, IMA J. Numer. Anal. 44 (2023), 2725–2751.
- [19] H. LIAO, X. ZHU, AND J. WANG, *The variable-step L1 scheme preserving a compatible energy law for time-fractional Allen-Cahn equation*, Numer. Math. Theor. Meth. Appl. 15 (2022), 1128–1146.
- [20] Y. LIN AND C. XU, Finite difference/spectral approximations for the time-fractional diffusion equation, J. Comput. Phys. 225 (2007), 1533–1552.
- [21] J. LIU AND H. FU, An efficient QSC approximation of variable-order time-fractional mobile-immobile diffusion equations with variably diffusive coefficients, J. Sci. Comput. 93 (2022), 44.
- [22] J. LIU, H. FU, X. CHAI, Y. SUN, AND H. GUO, Stability and convergence analysis of the quadratic spline collocation method for time-dependent fractional diffusion equations, Appl. Math. Comput. 346 (2019), 633–648.
- [23] J. LIU, H. FU, H. WANG, AND X. CHAI, A preconditioned fast quadratic spline collocation method for two-sided space-fractional partial differential equations, J. Comput. Appl. Math. 360 (2019), 138–156.
- [24] J. LIU, H. FU, AND J. ZHANG, A QSC method for fractional subdiffusion equations with fractional boundary conditions and its application in parameters identification, Math. Comput. Simulat. 174 (2020), 153–174.
- [25] J. LIU, C. ZHU, Y. CHEN, AND H. FU, A Crank-Nicolson ADI quadratic spline collocation method for two-dimensional Riemann-Liouville space-fractional diffusion equations, Appl. Numer. Math. 160 (2021), 331–384.
- [26] Y. Liu, N. Liu, H. Li, and J. Wang, Fast calculation based on a spatial two-grid finite element algorithm for a nonlinear space-time fractional diffusion model, Numer. Meth. Part. D. E. 36 (2020), 1904–1921.
- [27] W. Luo, T. Huang, G. Wu, and X. Gu, Quadratic spline collocation method for the time fractional subdiffusion equation, Appl. Math. Comput. 276 (2016), 252–265.

- [28] L. MA, H. FU, B. ZHANG, AND S. XIE, A fast compact block-centered finite difference method on graded meshes for time-fractional reaction-diffusion equations and its robust analysis, Numer. Math. Theor. Meth. Appl. 17 (2024), 429–462.
- [29] M. J. MARSDEN, Quadratic spline interpolation, Bull. Am. Math. Soc. 30 (1974), 903–906.
- [30] R. METLER, J. KLAFTER, AND D. C. MONTGOMERY, *The random walk's guide to anomalous diffusion: A fractional dynamics approach*, Phys. Reports 339 (2000), 1–77.
- [31] A. D. OBEMBE, M. E. HOSSAIN, AND S. A. ABU-KHAMSIN, *Variable-order derivative time fractional diffusion model for heterogeneous porous media*, J. Petrol. Sci. Eng. 152 (2017), 391–405.
- [32] Y. PACHEPSKY, D. TIMLIN, AND W. RAWLS, Generalized Richards' equation to simulate water transport in unsaturated soils, J. Hydrol. 272 (2003), 3–13.
- [33] Z. QIAO, Z. ZHANG, AND T. TANG, An adaptive time-stepping strategy for the molecular beam epitaxy models, SIAM J. Sci. Comput. 33 (2011), 1395–1414.
- [34] R. SCHUMER, D. BENSON, AND M. MEERSCHAERT, Fractal mobile/immobile solute transport, Water Resour Res. 39 (2003), 1–12.
- [35] M. STYNES, A survey of the L1 scheme in the discretisation of time-fractional problems, Numer. Math. Theor. Meth. Appl. 15 (2022), 1173–1192.
- [36] H. Sun, M. Meerschaert, Y. Zhang, J. Zhu, W. Chen, and Y. Chen, *A fractal Richards'* equation to capture the non-Boltzmann scaling of water transport in unsaturated media, Adv. Water Resour. 52 (2013), 292–295.
- [37] H. Sun, Y. Zhang, D. Baleanu, W. Chen, and Y. Chen, *A new collection of real world applications of fractional calculus in science and engineering*, Commun. Nonlinear Sci. Numer. Simulat. 64 (2018), 213–231.
- [38] Z. Sun and X. Wu, A fully discrete difference scheme for a diffusion-wave system, Appl. Numer. Math. 56 (2006), 193–209.
- [39] W. TIAN, H. ZHOU, AND W. DENG, A class of second order difference approximations for solving space fractional diffusion equations, Math. Comput. 84 (2015), 1703–1727.
- [40] H. WANG AND X. ZHENG, Wellposedness and regularity of the variable-order time-fractional diffusion equations, J. Math. Anal. Appl. 475 (2019), 1778–1802.
- [41] Z. WANG AND S. VONG, A high-order exponential ADI scheme for two dimensional time fractional convection-diffusion equations, Comput. Math. Appl. 68 (2014), 185–196.
- [42] X. YANG, H. ZHANG, AND Q. TANG, A spline collocation method for a fractional mobile-immobile equation with variable coefficients, Comput. Appl. Math. 39 (2020), 34.
- [43] W. Yuan, D. Li, and C. Zhang, Linearized transformed L1 Galerkin FEMs with unconditional convergence for nonlinear time tractional Schrödinger equations, Numer. Math. Theor. Meth. Appl. 16 (2023), 348–369.
- [44] F. ZENG, F. LIU, C. LI, K. BURRAGE, AND I. TURNER, A Crank-Nicolson ADI spectral method for a two-dimensional Riesz space fractional nonliear reaction-diffusion equation, SIAM J. Numer. Anal. 52 (2014), 2599–2622.
- [45] J. Zhang, Z. Fang, and H. Sun, Exponential-sum-approximation technique for variable-order time-fractional diffusion equations, J. Appl. Math. Comput. 68 (2022), 323–347.
- [46] Y. Zhang, C. Green, and B. Baeumer, Linking aquifer spatial properties and non-Fickian transport in mobile-immobile like alluvial settings, J. Hydrol. 512 (2014), 315–331.
- [47] Y. Zhang and Z. Sun, Alternating direction implicit schemes for the two-dimensional fractional sub-diffusion equation, J. Comput. Phys. 230 (2011), 8713–8728.
- [48] X. ZHENG, H. LIU, H. WANG, AND H. FU, Optimal-order finite element approximations to variable-coefficient two-sided space-fractional advection-reaction-diffusion equations in three space dimensions, Appl. Numer. Math. 161 (2021), 1–12.

[49] X. Zheng, H. Liu, H. Wang, and H. Fu, An efficient finite volume method for nonlinear distributed-order space-fractional diffusion equations in three space dimensions, J. Sci. Comput. 80 (2019), 1395–1418.

- [50] X. Zheng and H. Wang, Optimal-order error estimates of finite element approximations to variable-order time-fractional diffusion equations without regularity assumptions of the true solutions, IMA. J. Numer. Anal. 41 (2021), 1522–1545.
- [51] Y. Zhou and M. Stynes, Optimal convergence rates in time-fractional discretisations: the L1, $\overline{L1}$ and Alikhanov schemes, East Asian J. Appl. Math. 12 (2022), 503–520.